Nuclear accumulation of MKL1 in luminal breast cancer cells impairs genomic activity of ERα and is associated with endocrine resistance

Charly Jehanno, Tamara Fernández-Calero, Denis Habauzit, Stéphane Avner, Frédéric Percevault, Emmanuelle Jullion, Pascale Le Goff, Marie May Coissieux, Simone Muenst, Mónica Marín, et al.

▶ **To cite this version:**

Charly Jehanno, Tamara Fernández-Calero, Denis Habauzit, Stéphane Avner, Frédéric Percevault, et al.. Nuclear accumulation of MKL1 in luminal breast cancer cells impairs genomic activity of ERα and is associated with endocrine resistance. Biochimica et Biophysica Acta - Gene Regulatory Mechanisms , 2020, 1863 (5), pp.194507. 10.1016/j.bbagrm.2020.194507 . hal-02565572

HAL Id: hal-02565572

https://univ-rennes.hal.science/hal-02565572

Submitted on 7 May 2020

HAL is a multi-disciplinary open access archive for the deposit and dissemination of scientific research documents, whether they are published or not. The documents may come from teaching and research institutions in France or abroad, or from public or private research centers.

L'archive ouverte pluridisciplinaire **HAL**, est destinée au dépôt et à la diffusion de documents scientifiques de niveau recherche, publiés ou non, émanant des établissements d'enseignement et de recherche français ou étrangers, des laboratoires publics ou privés.

Nuclear accumulation of MKL1 in luminal breast cancer cells impairs genomic activity of ERα and is associated with endocrine resistance

Charly Jehanno[a,b,1], Tamara Fernandez-Calero[c,d,e,1], Denis Habauzit[a], Stephane Avner[f], Frederic Percevault[a], Emmanuelle Jullion[f], Pascale Le Goff[a], Marie May Coissieux[b], Simone Muenst[g], Monica Marin[c], Denis Michel[a], Raphaël Métivier[f] and Gilles Flouriot[a*]

[a] Univ Rennes, Inserm, EHESP, Irset (Institut de Recherche en Santé, Environnement et Travail) – UMR_S 1085, F-35000 Rennes, France

[b] University Hospital Basel, University of Basel, Basel, Switzerland

[c] Biochemistry-Molecular Biology, Facultad de Ciencias, Universidad de la República, Iguá 4225, 11400 Montevideo, Uruguay

[d] Bioinformatics Unit, Institut Pasteur Montevideo, Mataojo 2020, 11400 Montevideo, Uruguay

[e] Departamento de Ciencias Exactas y Naturales, Universidad Católica del Uruguay, Montevideo, Uruguay

[f] Univ Rennes, Institut de Génétique et Développement de Rennes, UMR 6290 CNRS, Rennes, France

[g] Institute of Medical Genetics and Pathology, University Hospital Basel, University of Basel, Basel, Switzerland

[1] Contributed equally to the work.

[*]To whom correspondence should be addressed: Dr. Gilles Flouriot, Irset, Inserm U1085, 9 rue du Prof. Léon Bernard, 35000 Rennes cedex, France ; Phone: +33-2 23 23 68 04 ; Fax: +33-2 23 23 67 94 ; E-mail: gilles.flouriot@univ-rennes1.fr

Running Title: MKL1 impairs genomic activity of ERα

Keywords: Breast cancer, Endocrine resistance, Estrogen receptor, MKL1, Gene regulation, Cistrome

Journal Pre-proof

Abstract

Estrogen receptor (ERα) is central in driving the development of hormone-dependent breast cancers. A major challenge in treating these cancers is to understand and overcome endocrine resistance. The Megakaryoblastic Leukemia 1 (MKL1, MRTFA) protein is a master regulator of actin dynamic and cellular motile functions, whose nuclear translocation favors epithelial-mesenchymal transition. We previously demonstrated that nuclear accumulation of MKL1 in estrogen-responsive breast cancer cell lines promotes hormonal escape. In the present study, we confirm through tissue microarray analysis that nuclear immunostaining of MKL1 is associated with endocrine resistance in a cohort of breast cancers and we decipher the underlining mechanisms using cell line models. We show through gene expression microarray analysis that the nuclear accumulation of MKL1 induces dedifferentiation leading to a mixed luminal/basal phenotype and suppresses estrogen-mediated control of gene expression. Chromatin immunoprecipitation of DNA coupled to high-throughput sequencing (ChIP-Seq) shows a profound reprogramming in ERα cistrome associated with a massive loss of ERα binding sites (ERBSs) generally associated with lower ERα-binding levels. Novel ERBSs appear to be associated with EGF and RAS signaling pathways. Collectively, these results highlight a major role of MKL1 in the loss of ERα transcriptional activity observed in certain cases of endocrine resistances, thereby contributing to breast tumor cells malignancy.

Abbreviations: ChIP-Seq: chromatin immunoprecipitation of DNA coupled to high-throughput sequencing; DMEM: dulbecco's modified Eagle's medium; E2: 17β-estradiol; ERα: estrogen receptor alpha; ERBS: ERα binding site; EMT: epithelial-mesenchymal transition; FCS: fetal calf serum; HER1: human epidermal growth factor receptor 1; HER2: human epidermal growth factor receptor 2 ; MaSC: mammary stem cell; MKL1: megakaryoblastic leukemia 1; MRTFA: myocardin-related transcription factor A; PR: progesterone receptor; SERM: selective estrogen receptor modulators; SRF: serum response factor; TNBC: triple-negative breast cancer.

1. Introduction

Breast cancers exhibit strong heterogeneity from genetic and phenotypic features to clinical behavior [1]. Based on global gene expression profiles, at least four major molecular subtypes have been identified, including luminal A, luminal B, HER2-enriched and basal-like tumor [2,3]. Estrogen receptor-alpha (ERα) expression defines the luminal subtypes. More than two-thirds of breast cancers overexpress ERα allowing most of them to depend on estrogen to proliferate [4,5]. This specificity makes ERα an ideal target for endocrine therapies that use selective estrogen receptor modulators (SERM) such as tamoxifen and/or aromatase inhibitors to block estrogen-dependent cell proliferation [6,7]. Unfortunately, a significant number of ERα positive breast tumors fail to initially respond to endocrine therapy or stop benefiting from such treatments and acquire resistance [8,9]. Endocrine resistance often relies on changes in the functional properties of ERα, whose activity may shift from ligand-dependent to ligand-independent activity [9]. Actually, luminal A breast cancers generally express higher level of ERα, exhibit better response to endocrine therapy and have better prognosis than luminal B subtype [10,11]. These last years, estrogen signaling in luminal breast cancer cells was deeply explored through gene expression and genome-wide chromatin binding profiling using both cell lines and human tumors [12–14]. Data highlighted that ERα binds to several thousand of sites across the genome and that most of these sites are located far away from the promoter regions. The genomic regions bound by ERα are enriched with cis-regulatory elements bound by pioneer factors, notably FOXA1 and GATA3 whose expression is correlated with luminal subtype [15]. ERα binding to chromatin still occurs in breast cancer cell lines and tumors that are resistant to antiestrogen therapies [14]. However, these cells do present a modified cistrome of ERα, having lost a number of ERα binding sites (ERBSs) but also harboring specific ones. Interestingly, these novel ERBSs found in antiestrogen-resistant cells, are still bound by FOXA1 but are depleted in GATA3 motifs. In addition, the ERα cistrome in drug resistant cell lines and tumors is characterized by an increased average ERα binding signal intensity likely resulting from a constitutively active estrogen receptor. The transcriptomic signature of these cells remains associated with ERα-positive luminal subtype [14]. More aggressive in nature, with higher proliferation and metastasis potential than luminal subtypes, basal-like tumors often have a triple ERα/progesterone receptor (PR)/HER2 negative phenotype [2,16]. Consequently, these tumors are not amenable to conventional targeted therapies. Recent studies suggest that basal-like breast cancers originate from luminal cells rather than a mammary stem cell (MaSC) [1,17,18]. Up to 30% of initially ERα-positive tumors that have developed

resistance to antiestrogen therapies lose part of ERα expression [19]. Therefore, endocrine resistance may also rely on a dedifferentiation process leading luminal cancers to switch to an ERα-negative phenotype.

MKL1, also called MRTFA, MAL or BSAC, is a member of the myocardin-related transcription factor (MRTF) family, whose members are coactivators of the serum response factor (SRF) [20,21]. Its main role is to sense the degree of actin polymerization controlled by Rho GTPases and to subsequently integrate this information at the gene expression level through a nuclear translocation [20]. As a master regulator of cellular motile and contractile functions, MKL1 exerts important roles in vascular smooth muscle cell and cardiac myocyte differentiation, and neuronal migration [21]. In mammary gland, MKL1 is essential for the basal/myoepithelial cell differentiation and function [22,23]. During tumorigenesis, MKL1 is required for tumor cell invasion and metastasis mediating the adaptive changes in cell shape, adhesion, and migration linked to the actin cytoskeleton [24]. Recent genome-wide association studies have identified MKL1 locus as a susceptible risk factor for breast cancer and especially triple-negative breast cancer (TNBC) [25–27]. We previously showed that the activation of MKL1 in estrogen sensitive breast cancer cell lines leads to hormonal resistance and reduced expression of ERα, PR and HER2, recalling the triple negative phenotype [28]. In the present study, we show that nuclear accumulation of MKL1 is associated with endocrine resistance in a cohort of breast cancers. Using genome wide analysis of gene expression and ERα chromatin binding, we demonstrate that, upon the expression of a constitutively active form of MKL1, initially ERα-positive breast cancer cells initiate a dedifferentiation process associated with a profound reprogramming in ERα cistrome leading to hormonal escape.

Journal Pre-proof

2. Materials and Methods

2.1. Cell culture and transfection

Stably transfected MCF7 T-Rex sub-clones (T-Rex system, Invitrogen), MCF7-control (with empty pcDNA4/TO expression vector) and MCF7-MKL1ΔN200 (with MKL1ΔN200 pcDNA4/TO expression vector), were previously described [28,29]. MCF7 T-Rex sub-clones as well as MCF10A, T47D, ZR-75-1, MCF7 AKT+ [express myr-akt1 (activated) plasmid (Upstate cell signaling solutions)], MDA-MB-468, MDA-MB-231 and SUM159PT cell lines were routinely maintained in DMEM (Invitrogen) supplemented with 10% fetal calf serum (FCS) (Biowest) and antibiotics (Invitrogen) at 37ºC in 5% CO_2. Before any experiments, cells were grown in phenol red-free DMEM (Invitrogen) containing 2.5% charcoal-stripped FCS (Biowest) for at least 72 hours. In order to induce the expression of the constitutively active mutant of MKL1 (MKL1ΔN200), MCF7 cells were treated the last 48 hours with 1 µg/mL tetracycline. Tetracycline treatment was systematically performed on both MCF7-control and MCF7-MKL1ΔN200 cells. 17β-estradiol (E2, Sigma-Aldrich), 4-hydroxytamoxifen (OHT, Sigma-Aldrich) and ICI 182,780 (ICI, Sigma-Aldrich) were used at a final concentration of 1 or 10 nM, 1000 nM and 100 nM, respectively. Jasplakinolide (Abcam) and Erlotinib (Sigma-Aldrich) were used at the final concentration of 0.5 µg/ml and 100 µM, respectively. Transient transfection experiments were performed with the reporter gene C3 (complement 3)-Luc, the pCR-ERα expression vector, p3Xflag-MKL1 ΔN200 and the CMV-βgal internal control as previously described [28,30].

2.2. Matrigel invasion assay

3D spheroids of breast cancer cell lines were formed in untreated plastic petri dishes by constant gyratory shaking at 60 r.p.m. as previously described [31]. Matrigel solution was prepared in culture medium at the final concentration of 1mg/ml. Resuspended in Matrigel solution, spheroids were then seeded in on the top of a matrigel cushion already formed in 96- well plates. To monitor cell invasion of Matrigel, images were taken every 24 hours by microscopy (DMIRB-Leica) and the size of the cellular spreading zone was calculated using Image J software.

2.3. Protein extraction and western blotting

Whole-cell extracts were directly prepared in 3X Laemmli buffer. Following sonication, the protein extracts were denatured for 5 min at 95°C, separated on 10 % SDS polyacrylamide gels, and transferred to polyvinylidene difluoride membrane (Millipore). Western blots were performed as previously described

[28,29] using the primary antibodies against MKL1 (ab14984) from Abcam, ERα (sc-543) and p-ERK (sc-7383) from Santa Cruz Biotechnology, HER1 (SAB1405746) and β actin (A1978) from Sigma-Aldrich and p-Akt (4060), Akt (9272) and ERK 1/2 (4695) from Cell signaling technology.

2.4. Immunofluorescence and immunohistochemical analysis

For cell lines, cells were grown on 10 mm-diameter coverslips in 24-well plates. After treatment, cells were fixed with phosphate-buffered saline (PBS) containing 4% paraformaldehyde (PAF) for 10 min and then permeabilized in PBS containing 0.3% Triton X-100 for 10 min. Incubation with the primary antibody (1/1000) was performed overnight (ON) at 4°C. Primary antibodies against N-cadherin (N19, sc-1502), P-cadherin (H105, sc-7893), cytokeratin 14 (LL02, sc-58724), cytokeratin 18 (C-04, sc-51582), ERα (C-terminal, HC-20, sc-543), GATA3 (sc-22206) and HER1 (1005, sc-03) were purchased from Santa Cruz Biotechnology. Antibodies directed against E-cadherin (ab15148), alpha smooth muscle actin (ab5694), MKL1 (ab14984), FOXC1 (ab5079), FOXA1 (ab23738), P300 (ab14984) and HER2 (ab16901) were obtained from Abcam. Anti-vimentin (clone V9) antibody was purchased from Sigma-Aldrich Primary antibody against ERα (N-terminal, 6F11) was purchased from Thermo Fisher Scientific. Dye-conjugated secondary antibodies (Abcam) were incubated 1h at room temperature. The cover slides were mounted in Duolink II mounting medium with DAPI (Sigma-Aldrich), images were obtained with an ApoTome Axio Z1 Imager microscope (Zeiss) and processed with Axio Vision Software. Fluorescence was quantified with ImageJ software from images obtained with identical exposure times. Immunofluorescence was scored for at least 20 cells per image on n images obtained from diverse experiments. The means obtained for every image were then averaged.

For MKL1 and ERα co-labeling experiments on tissue sections, paraffin-embedded tissues were cut at 4 µm, mounted on positively charged slides and dried at 58°C for 60 minutes. Immunohistology staining was performed on the Discovery XT Automated IHC stainer using the Ventana detection kit and Discovery Rhodamine and FAM kits (Ventana Medical Systems, Tucson, Ariz). Primary antibodies were anti-ERα (6F11, Thermo Fisher Scientific) and anti-MKL1 (HPA030782, Sigma-Aldrich).

For the immunohistchemical analysis, MKL1 staining on tissue microarrays (TMA) from breast cancer was performed using a Ventana Benchmark Discovery instrument (Roche Diagnostics). 4uM sections of the TMA blocks were pretreated with CC1 for 40 min. Then, slides were incubated with MKL1 primary antibody (ab14984, Abcam) at a dilution of 1:50 for 1h, followed by secondary antibody incubation and detection.

Hematoxylin II and bluing reagent (Ventana, Roche diagnostics) were used for counterstaining. Samples were scored as positive when the number of cells per sample displaying nuclear localization of MKL1 was superior to 30% or as low positive/negative when this number was below 30%. The blinded analysis of MKL1 expression was performed two times on two independent MKL1 staining of the TMA slides. For immunohistochemistry sections, images were captured using a Nikon Ni-e upright microscope coupled to a PRIOR slide loader. Acquisitions were performed with a 10x AIR objective with a DS-Fi3 camera using NIS software. Written informed consent was obtained from patients and the institutional ethics committee approved the study.

2.5. RNA extraction, gene expression array and RT-PCR assays

RNA purifications were performed immediately after a treatment of MCF7 cells with 10 nM E2 or ethanol (vehicle control) for 4h. RNAs were extracted with the RNeasy kit (Quiagen) and the quantity and quality of RNAs were assessed using a Nanodrop 1000 spectrophotometer (Nanodrop technology) and an Agilent Bioanalyser. RNAs were then reverse-transcribed and the obtained cDNA were amplified and Cy3-labelled according to the manufacturer's instructions (Agilent Technologies). Gene expression profiling was carried out on Agilent Whole Human Genome 8x60K Microarrays (Agilent Technologies) at the Biosit Rennes facility. Four independent RNA samples per condition (n=4) were randomly examined. Data analysis was performed using 'R' (R Foundation for Statistical Computing, Vienna, Austria), mainly through packages included in the Bioconductor suite [32]. Probes were filtered considering saturation, signal above background and uniformity. Only those with no replicate flagged in at least one condition were taken into account for data analysis. Samples were normalized using 75-percentile shift normalization. Gene expression values were computed as the median intensity values of all filtered probes design for each particular gene. Differential expression was assayed using the limma software package [33]. When we compared MCF7-MKL1ΔN200 and MCF7-control cells, genes were considered differentially expressed when the multiple testing adjusted *P*-value was <0.01 and the absolute value of fold change greater than 4. When we analyzed E2 transcriptional regulation, genes were considered differentially expressed when the multiple testing adjusted *P*-value was <0.05 and the absolute value of fold change greater than 1.8. Gene Ontology analysis and Kegg pathways enrichment analysis were conducted with clusterProfiler [34]. Up-regulated and down-regulated genes were used independently in these analyses. Quantitative RT-PCRs were performed as previously described [28]. Primers for RT-PCR are provided in Supplementary Materials **(Table S1)**.

2.6. Chromatin immunoprecipitation (ChIP)

MCF7 cells were treated with 10 nM E2 or ethanol (vehicle control) during 50 min, washed twice with PBS and cross-linked for 10 min with 1.5% formaldehyde (Sigma). The cross-link reaction was stopped with 0.125 M glycine for 1 min and cells were washed twice with PBS, scraped into 500 µl PBS with protease inhibitors (Complete Inhibitors, Roche), spun 2 min at 3000 g and snap frozen to -80°C. After cell lysis in 300 µl of lysis buffer [10 mM EDTA, 50 mM Tris-HCl (pH 8.0), 1% SDS, 0.5% Empigen BB detergent], ChIP was performed as previously described [35,36]. Antibodies against ERα (HC-20, sc-543, Santa Cruz Biotechnology), H3K27ac (ab4729, Abcam) and H3K4me2 (07-030, Merk Millipore) were used in this assay. DNA was purified on NucleoSpin columns (Macherey-Nagel) using NTB buffer. ChIP experiments were performed from at least five biological independent replicates. Primers used for real-time PCR are provided in Supplementary Materials **(Table S1)**.

2.7. ChIP-sequencing (ChIP-Seq) and ChIP-Seq data analysis

We pooled DNA originating from at least 18 different ChIP experiments conducted as described above. The ChIP DNA was prepared into libraries and sequenced using an Illumina HiSeq apparatus at the GenomEast platform (Institut de Génétique et de Biologie Moléculaire et Cellulaire; Strasbourg, France). Pooled control inputs DNA were processed in parallel. Reads were aligned onto the indexed chromosomes of the human hg19 (GRCh37) genome using bowtie 0.12.7 [37], allowing at most two mismatches (parameters –n 2; -l 28; -m 1 with --best and --strata options). Sequencing statistics are given in **Table S2**. Samtools 0.1.12a [38] implemented under galaxy (https://usegalaxy.org/) were used to generate signal files. Duplicate reads were removed using the rmDupBam tool, and GCbias were subsequently corrected by the compute/correct GC bias algorithms included in the DeepTools package. MACS 2.1.1.2016 [39] was then used for converting signal into .wig files and peak calling using low/up mfold bound adjusted to 5 and 50 respectively and at different *P*-values cutoff, as previously performed [35]. Input control file was used as reference for these peak-callings. The obtained .bed files corresponding to the genomic coordinates of identified ERα BSs were subsequently filtered against the lists of repetitive sequences obtained from the UCSC (blacklist; http://genome.ucsc.edu/cgi-bin). Regions exhibiting high background signal generated by a poor normalization to input due to excessive sequences overrepresentation (consecutive of the highly rearranged genome of MCF7 cells) were also removed. ER-bound identified genomic regions are provided in the **Table**

S3. For alignment and calculations of mean signals at precise subset of genomic regions, we corrected the bias of diverging sequencing depths between different samples by normalizing the signal intensities of a given .wig to the one with the highest sequencing depth. Motifs analyses were performed using the CentDist (http://biogpu.ddns.comp.nus.edu.sg/~chipseq/webseqtools2) and SeqPos (http://cistrome.org/ap/ [40]) algorithms. All other integrative analyses of the ChIP-Seq data were performed using home-made scripts and algorithms from the cistrome web-platform (http://cistrome.org/ap/).

2.8. Availability of data

The microarray and ChIP-Seq data generated in this study have been submitted to the NCBI Gene Expression Omnibus website (http://www.ncbi.nlm.nih.gov/geo/)[41] under accession No. GSE 107924 and GSE 107476, respectively.

Journal Pre-proof

3. Results

3.1. Nuclear accumulation of MKL1 favors invasiveness and impairs transactivation efficiency of ERα

We previously showed that breast cancer cell lines exhibit different MKL1 activity [28]. As shown in **Fig 1A** and **Fig S1A**, MKL1 is almost cytoplasmic and inactive in luminal ERα-positive breast cancer cell lines such as MCF7, T47D or ZR-75-1, which exhibit a well-differentiated epithelial phenotype. In the non-tumorigenic epithelial cell line MCF10A, the vast majority of cells exhibit a cytoplasmic localization of MKL1. Only cells on islet periphery present a nuclear translocation of MKL1. Similarly, a slight onset of nuclear accumulation of MKL1 is observed in the endocrine resistant ERα-positive breast cancer cell line expressing a constitutively active form of AKT (MCF7 AKT+). Finally, all cell lines having an epithelial-mesenchymal transition (EMT) phenotype such as MDA-MB-468, MDA-MB-231 or SUM159PT display MKL1 nuclear localization (**Fig. 1A**). While MKL1 has a different localization in these different cell lines, its expression level measured by Western blot remains similar (**Fig S1B**). The invasive capability of the different cell lines was then tested on 3D cell culture using a Matrigel Invasion assay (**Fig. 1B**). Results clearly show a positive correlation between the nuclear localization of MKL1 and invasiveness. As expected, the basal-like cell lines MDA-MB-231 and SUM159PT strongly invade the Matrigel while ERα-positive breast cancer cell lines are noninvasive. Although we were unable to measure the invasive capability of the MDA-MB-468 due to their inability to form spheroids, this cell line is known to be highly invasive in the literature. Transactivation efficiency of the estrogen receptor on an ERE-driven reporter gene was evaluated in parallel through transient transfection experiments in these different cell lines. Importantly, we observed that the transactivation activity of ERα was the strongest in the ERα-positive breast cancer cell lines and dramatically lower in the nuclear MKL1-positive invasive cell lines MDA-MB-468, MDA-MB-231 or SUM159PT (**Fig. 1C**). These correlative data suggest a close link between MKL1 nuclear translocation, invasiveness and impaired ERα transactivation efficiency. To shift from correlation to causality, we investigated whether nuclear accumulation of MKL1 in ERα-positive breast cancer cell lines, using a MKL1 mutant or a drug inducing MKL1 translocation, could impact invasiveness and ERα transactivation efficiency. We previously established a MCF7 cell line expressing a N-terminal deleted mutant of MKL1 (MKL1 ΔN200) devoid of the RPEL motifs (actin binding sites), allowing permanent translocation and constitutive activity of MKL1 into the nucleus [28,29] (**Fig. 1D**). As shown in **Fig. 1E** and **Fig S1C**, the expression of this MKL1 ΔN200 mutant triggered Matrigel invasion by MCF7 cells. This invasion was partly slowed down in presence of E2. Finally, transactivation efficiency of ERα was measured in MCF7 and T47D after either transiently expressing of MKL1 ΔN200 mutant or treating cells with

jasplakinolide, a commonly used actin filament polymerization and stabilizing drug, which induces MKL1 nuclear translocation (**Fig. 1D**). As shown in **Fig. 1F**, both approaches provoke a significant decrease in ERα transactivation efficiency of the reporter gene, reaching levels similars to those observed in naturally nuclear MKL1-positive invasive cell lines. Altogether, these results obtained using complementary approaches show that the nuclear translocation of MKL1 favors invasiveness and impairs transactivation efficiency of ERα.

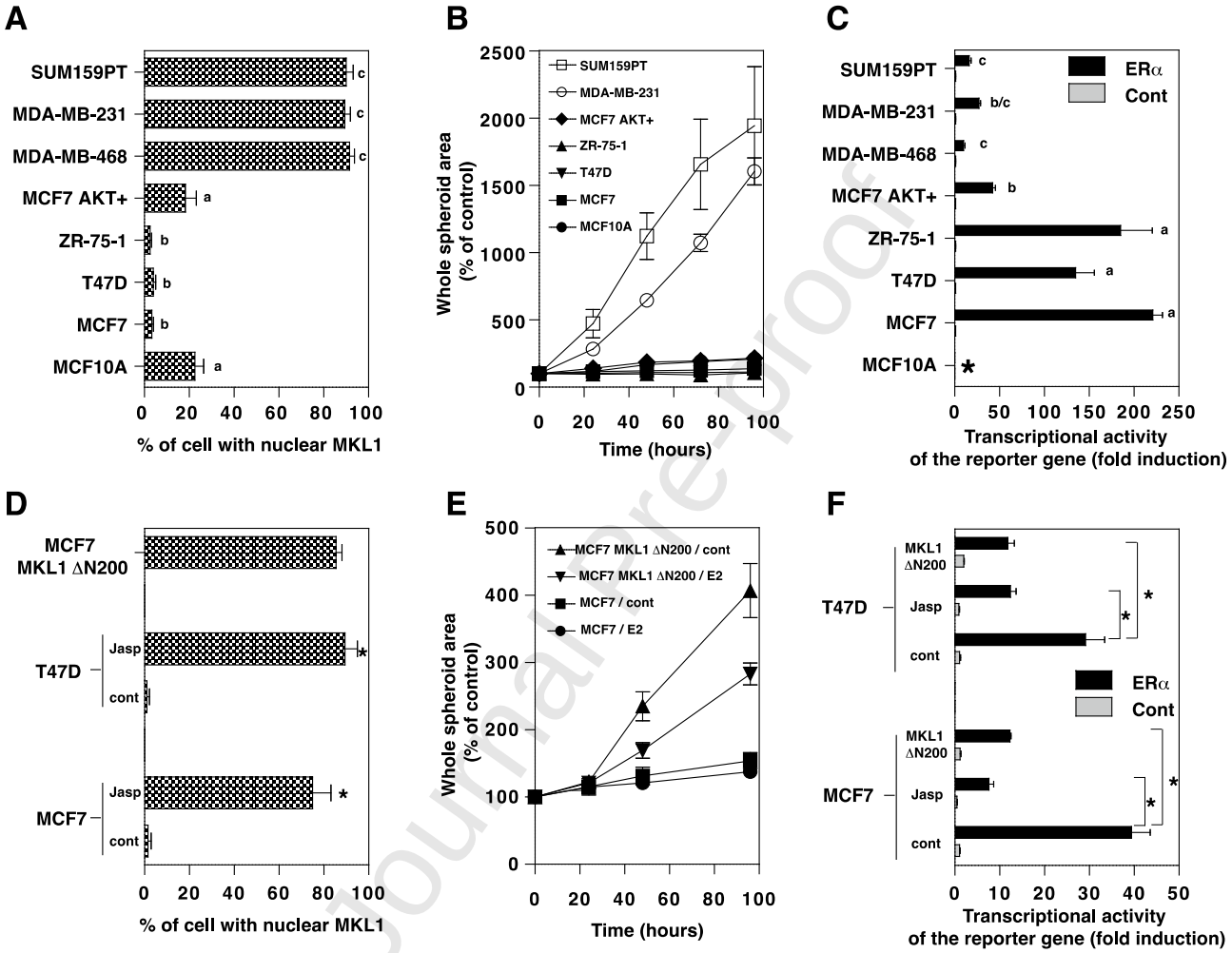

Fig. 1. Nuclear accumulation of MKL1 favors invasiveness and impairs the transactivation efficiency of ERα. Were analyzed the non-tumorigenic epithelial cell line MCF10A, the ERα-positive breast cancer cell lines MCF7, T47D and ZR-75-1 (luminal A subtype), the ERα-positive breast cancer cell line MCF7 expressing a constitutively active form of AKT (endocrine resistant cell line) and the triple negative breast cancer cell lines MDA-MB-468, MDA-MB-231 and SUM159PT (basal-like subtype). (A) MKL1 expression and localization were analyzed by immunofluorescence in the different cell lines and the percentage of cells with nuclear MKL1 staining was then quantified (mean values from at least 30 images ± SEM). Columns with different superscripts differ significantly ($p<0.01$, student 's *t*-test). (B) A 3D spheroid cell invasion assay in Matrigel

was performed on the different cell lines. Images were taken every 24 hours by microscopy and the diameter of the spreading spheroid was measured using Image J software. Data corresponds to the mean ± SEM from at least 10 different experiments and are expressed in percentage referring to the diameter measured at day 0. (C) Cells were transiently transfected with the C3-LUC reporter gene (100 ng), the ERα expression vector (50ng) and the internal control CMV-βgal (100ng). Cells were then treated for 24h with E2 and the luciferase activities were measured and normalized to β-galactosidase activities. Data corresponds to the mean values from at least triplicate experiments ± SEM and are expressed as fold change from the control. Columns with different superscripts differ significantly ($p<0.01$, student 's *t*-test). ° Transfection was ineffective in MCF10A. (D) Percentage of cells with nuclear MKL1 staining in MKL1 ΔN200 MCF7 cells treated 48h with tetracycline (1μg/ml) or in MCF7 and T47D cells treated or not with jasplakinolide (0.5 μg/ml) (mean values from at least 10 images ± SEM) ($p<0.05$). (E) 3D spheroid cell invasion assay in Matrigel of tetracycline-treated control and MKL1 ΔN200 MCF7 cells with or without E2 (10 nM). (F) MCF7 and T47D cells were transfected as in panel C in the presence or the absence of MKL1 ΔN200 expression vector and then treated or not with jasplakinolide in the presence of E2. Data are the mean values from triplicate ± SD and are expressed in fold change compared to the control ($p<0.05$, student 's *t*-test).

3.2. Nuclear accumulation of MKL1 is associated with endocrine resistance in breast cancers.

Above results associates the nuclear localization of MKL1 in breast cell lines with de-differentiation and invasive processes. To evaluate the physiopathological relevance of this finding, we next extended our study to healthy and cancerous human breast tissues. As illustrated in **Fig. 2A**, immunofluorescence experiments confirm that the transcriptional coactivator MKL1 is active and expressed in the nucleus of basal/myoepithelial cells while ERα is present in a small number of luminal cells in healthy breast tissues [4,22,23]. Nuclear co-localization of the two proteins was not observed in healthy human mammary gland. In contrast, a nuclear co-localization of ERα and MKL1 proteins was detected in ERα-positive malignant tumors where some ERα-positive cells begin to express high level of nuclear MKL1 (**Fig. 2A**). In light of these results, we performed an immunohistochemical analysis of MKL1 protein expression on a tissue microarray encompassing 130 breast cancer patient samples and covering every breast tumor subtypes (**Fig. 2B and Table S4**). We quantified the percentage of cells displaying nuclear localization of MKL1 in each sample. We first detected a significant increase in the number of MKL1 nuclear positive (NP) cells in tumor tissue compared to adjacent non-tumor tissue, except for the ER+/PR+/HER2- subtype (**Fig. 2C**). Then we aimed

to evaluate whether ERα positive breast tumors clinically described as hormone therapy refractory could be discriminated based on the their abundance in cells showing nuclear MKL1. Samples were split in two groups, MKL1 high or MKL1 weak/negative. In the 41 cases for which the status hormone therapy status was available, we detected a significant increase of MKL1-high tumors (**Fig. 2D**), indicating that the nuclear localization of MKL1 is associated with hormone resistance in our cohort.

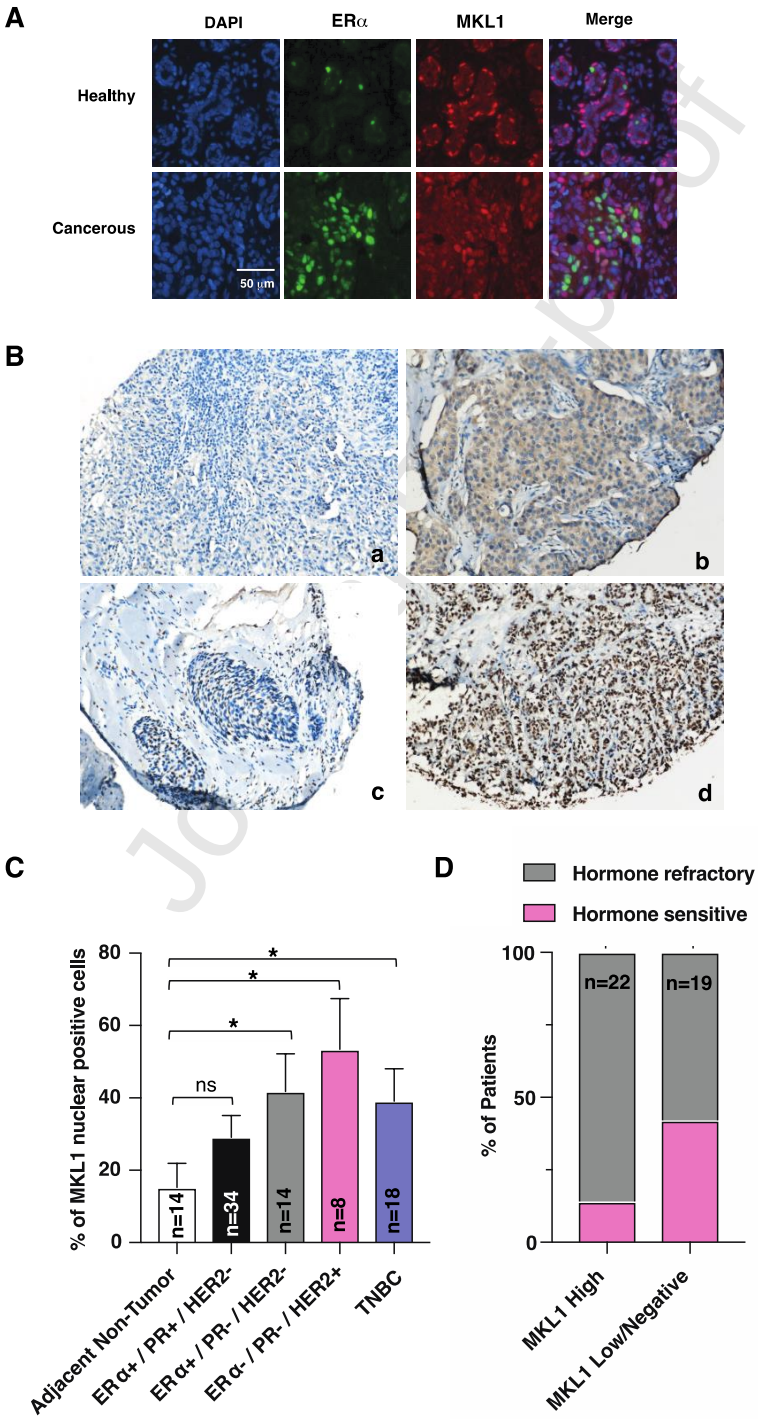

Fig. 2. Nuclear accumulation of MKL1 is associated with endocrine resistance in breast cancers. (A) Detection of ERα and MKL1 proteins by immunoflorrescence in healthy and ER-positive grade III breast cancer cells. In healthy tissue, ERα is expressed in few luminal cells while MKL1 is located in myoepithelial cells. In the tumor, some breast cancer cells co-expressed ERα and MKL1 proteins. Nuclei were stained with DAPI. (B) Representatives images of MKL1 immunohistochimical staining across different human tumor samples. (a) refers to as a MKL1 negative sample, (b) shows a cytoplasmic localization of MKL1, therefore considered as MKL1 nuclear negative staining (c) shows a weakly fraction of MKL1 nuclear positive (NP) cells, therefore also considered as MKL1 negative, (d) shows a MKL1 nuclear positive staining. (C) Quantification of MKL1 NP cells per breast cancer subtype, compared to adjacent non tumor tissue. *p-value <0.05, with a student t-test compared to the control, ns: non-significant. (D) MKL1 nuclear staining according to hormone therapy responsiveness status. ERα+ PR+/- (HER2 -) tumor samples were subdivided into two categories according to MKL1 staining. Samples harboring more than 30% of MKL1 NP cells were considered as MKL1 high whereas samples harboring less than 30% of MKL1 NP cells were considered as low or negative. Hormone refractory status comprises both innate and acquired lack of responsiveness to hormone therapy. *p-value <0.05, with a Chi-square test.

3.3. Nuclear accumulation of MKL1 in MCF7 cells induces a mixed luminal/basal phenotype

In order to better understand how MKL1 could promote endocrine resistance, we aimed at studying the consequences of MKL1 activation in ERα-positive breast cancer cells using unbiased approaches. We previously showed that actin-cytoskeleton remodeling and nuclear accumulation of MKL1 using the MKL1 ΔN200 mutant, abolishes the E2-dependent proliferation of MCF7 cells and impairs estrogen mediated regulation of few ER-target genes [28]. To further explore the changes in gene signature induced by the MKL1 mutant, we analyzed the gene expression profiles of MCF7 MKL1 ΔN200 and MCF7 control cells through microarray experiments. We defined a set of differentially expressed genes setting an arbitrary cut-off of adjusted *P*-value < 0.01 and a fold change > ±4 (**Table S5**). This threshold resulted in a set of 1,016 up-regulated and 976 down-regulated genes in MCF7 MKL1 ΔN200 as compared to MCF7 control cells. Functional analysis revealed an overrepresentation of genes involved in cell adhesion, ECM-receptor interactions, actin cytoskeleton organization and migration as well as genes involved in kinase cascades and signal transduction upon MKL1 ΔN200 signaling (**Fig. 3A** and **Table S6**), functions that are consistent with the induction of EMT [42]. Furthermore, we found an underrepresentation of genes involved in epigenetic

modulations such as chromatin remodeling or DNA methylation, processes that have been also associated with EMT [43,44].

Because patterns of gene expression allow classifying breast tumors according to major molecular subtypes, we next investigated the expression of subsets of genes that are distinctive of clinically relevant breast cancer subgroups. We selected 48, 37 and 11 genes which have been associated to basal-like, luminal and HER2-overexpressing tumors, respectively [3,45,46] (**Table S7**), and performed a gene set enrichment analysis. The analysis revealed a significant association of MCF7 control and MKL1 ΔN200 cells to the luminal and to the basal markers gene set, respectively (**Fig. S2A)**. No significant association was observed to the HER2 markers gene set.

Hence, the microarray analysis described above evokes a partial transition of MCF7 MKL1 ΔN200 cells from a luminal to a basal-like phenotype. To further strengthen this observation, we performed immunocytology staining of certain basal-like biomarkers such as cytokeratin 14, P-cadherin, N-cadherin, vimentin, alpha actin and the human epidermal growth factor 1 (HER1), and confirmed their up-regulation in MKL1 ΔN200 cells (**Fig. 3B** and **Fig. S2B**). Moreover, FOXC1, the main transcription factor regulating EMT in basal-like breast cancers [47], was also strongly up-regulated in these cells. Among luminal biomarkers, cytokeratin 18 staining was not affected, E-cadherin exhibited a disrupted network and the luminal pioneer factor GATA3 was drastically repressed. The expression level of ERα dropped by 60%, reaching a level comparable to the one observed in control MCF7 cells treated with E2. Interestingly, the pioneer transcription factor FOXA1 exhibited a different pattern with a clear increase of its expression in MCF7 MKL1 ΔN200 cells. Finally, the expression level of HER2 was inhibited by the constitutively active form of MKL1.

Altogether, these results clearly show that an increased nuclear-translocation and activity of MKL1 shift the phenotypical features of MCF7 cells from a luminal to luminal/basal hybrid phenotype.

Journal Pre-proof

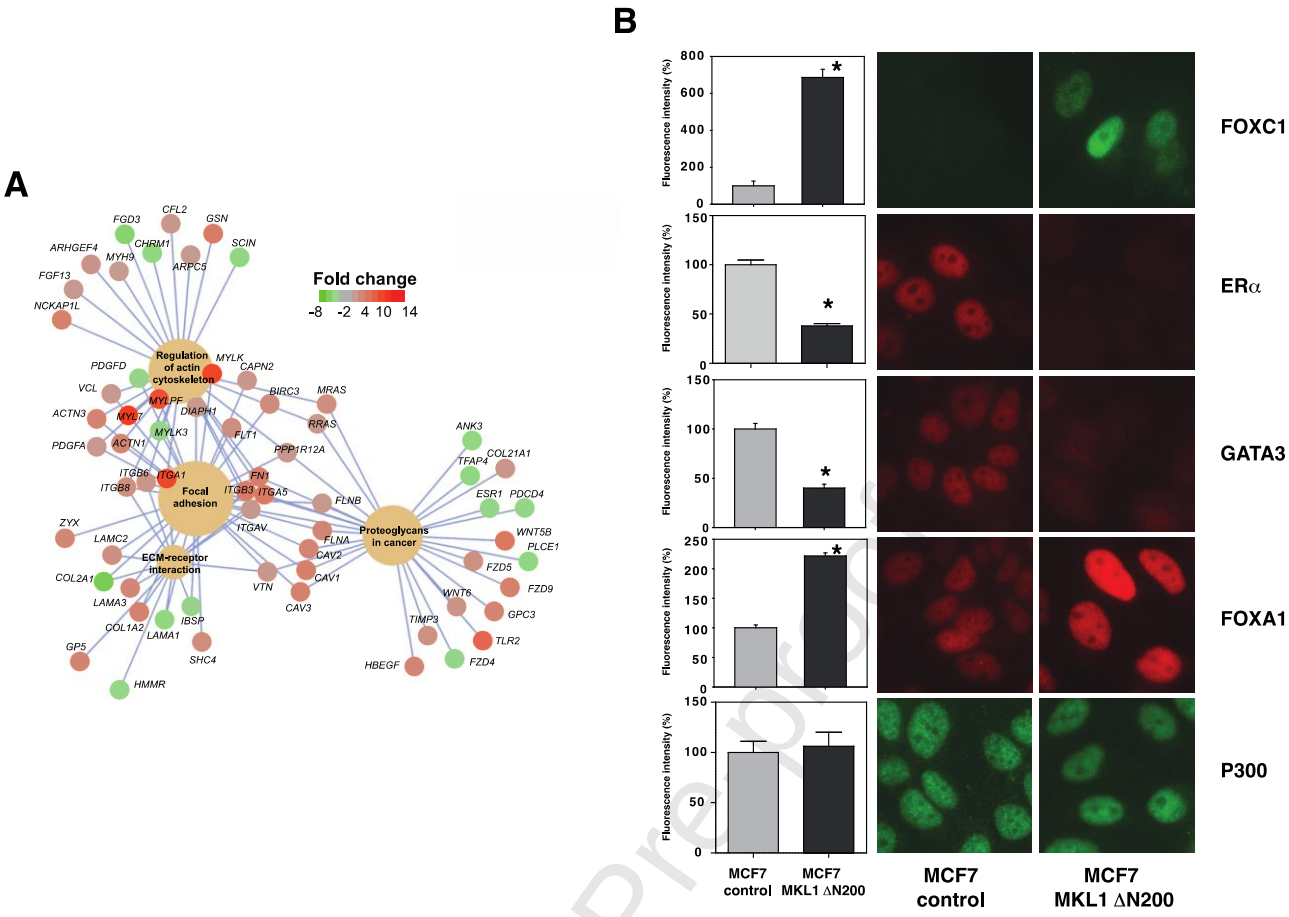

Fig. 3. Nuclear accumulation of MKL1 in MCF7 cells induces a mixed luminal/basal phenotype. The transcriptional profiles of control and MKL1 ΔN200 MCF7 cells were compared through microarray analysis. (A) Enriched Kegg pathways in our dataset are shown alongside the differentially expressed genes [showing P<0.01 and abs(FC)>4] involved. Genes are colored according to their log2FC expression values. (B) Immunofluorescence pictures of FOXC1, ERα, GATA3, FOXA1 and P300 after 48 hours of tetracycline treatment of control and MKL1 ΔN200 MCF7 cells. Densitometry quantification of the immunofluorescence expressed as percentage of the intensity measured in control MCF7 cells is shown on the left side of the panel. Error bars represent SEM (n ranges from 10 to 20; P<0.01, Student 's *t*-test).

3.4. MCF7 cells with a nuclear translocation of MKL1 lose E2 transcriptional regulation

In order to monitor estrogen signaling changes after MKL1 nuclear translocation, we used a microarray-based transcriptome analysis to identify E2-regulated genes in MCF7 MKL1 ΔN200 *versus* control cells treated for 4h with E2 or ethanol as vehicle control. We performed a differential gene expression (DE) analysis and selected an arbitrary cutoff of adjusted *P*-value < 0.05 and fold change > ±1.8 to define DE

genes (**Table S8**). Differential gene expression analysis evidenced 225 estrogen-regulated genes in control cells when treated with E2 (**Fig. 4A**; 185 up-regulated and 40 down-regulated). Ontology and pathway enrichment analysis of these genes revealed some terms and pathways previously described as E2-regulated in MCF7 cells, such as localization, cell communication and pathways in cancer [48] (**Table S9**). Strikingly, only 2 up-regulated genes were found in E2-treated MCF7 MKL1 ΔN200 and none were repressed by E2 (**Fig. 4A**). In general, the average of the fold-changes of the 185 up-regulated genes in control cells dropped from 2.3 to 1.2 in MCF7 MKL1 ΔN200 cells, while the one of the 40 down-regulated genes increased from 0.5 to 0.87. These data indicate that MCF7 MKL1 ΔN200 almost lose E2 transcriptional regulation.

We next addressed among the 225 E2-regulated genes whether some of them have modified basal expression due to MKL1 ΔN200 nuclear translocation and whether this could be correlated to the loss of their estrogenic response. Among these genes, 109 presented changes in their expression in the absence of ligand, including approximately half of the E2 up-regulated and E2 down-regulated genes. We categorized these 109 mRNAs in 4 categories depending upon the fold changes of their basal expression and of their response to E2 in control MCF7 cells. As shown within **Fig. 4B and 4C**, the E2 up-regulated genes in control cells were distributed equally between those whose basal expression is down-regulated and those whose basal expression is up-regulated in MCF7 MKL1 ΔN200 cells (C2 and C4 categories in **Fig. 4B and 4C**). In contrast, the basal expression of the majority of the E2 down-regulated genes in control cells (C1 and C3) were also down-regulated in the presence of MKL1 ΔN200, which might indicate a correlation between E2 and MKL1 effects for the E2 down-regulated genes only.

The expression profile of some E2-regulated genes from the clusters C1, C2 and C4 in MCF7 MKL1 ΔN200 and control cells was confirmed by quantitative RT-PCR (**Fig. S3**). Furthermore, these experiments show that MKL1 ΔN200-induced changes in basal expression of the genes were insensitive to antiestrogen treatments (**Fig. S3**). It should be noted that both antiestrogens used, the 4-hydroxytamoxifen (OHT) and ICI 182,780 (ICI), inhibit residual E2-induced activity of *GREB1* gene in MCF7 MKL1 ΔN200 cells, demonstrating the preservation of their antiestrogenic activity in these cells. Similar results were obtained on an ERE-driven reporter gene in transient transfection experiments (**Fig. S3C**). To confirm the link between MKL1 localization and these change in the expression of E2-regulated genes in different ERα-positive breast cancer cell lines, we used a complementary approach, in which MCF7 and T47D cells were treated with jasplakinolide drug leading to a nuclear translocation of MKL1 (**Fig. 1 and S1**). Results clearly show similar

expressions between the two cell lines and reproducible regulations regardless of how MKL1 nuclear translocation is induced. However, the amplitude of the effects was less marked after jasplakinolide treatment than after MKL1 ΔN200 expression (**Fig. S4**).

Finally, gene ontology and pathway enrichment analysis of the categories of genes could not be achieved due to the limited number of genes included in each subgroup. However, it should be noted that some genes generally considered as hallmarks of hormone-resistant breast cancer cells exhibited changes in expression, which could be expected to lead to such a cell phenotype. This is for instance the case of genes encoding the transcription factor FOXC1 and the growth factor AREG (amphiregulin) included in the C2 category of genes whose expression is up-regulated both by E2 and MKL1 ΔN200 and the chemokine CXCL12 in the category of genes (C4) in which MKL1 ΔN200 strongly counteracts the stimulating effect of E2.

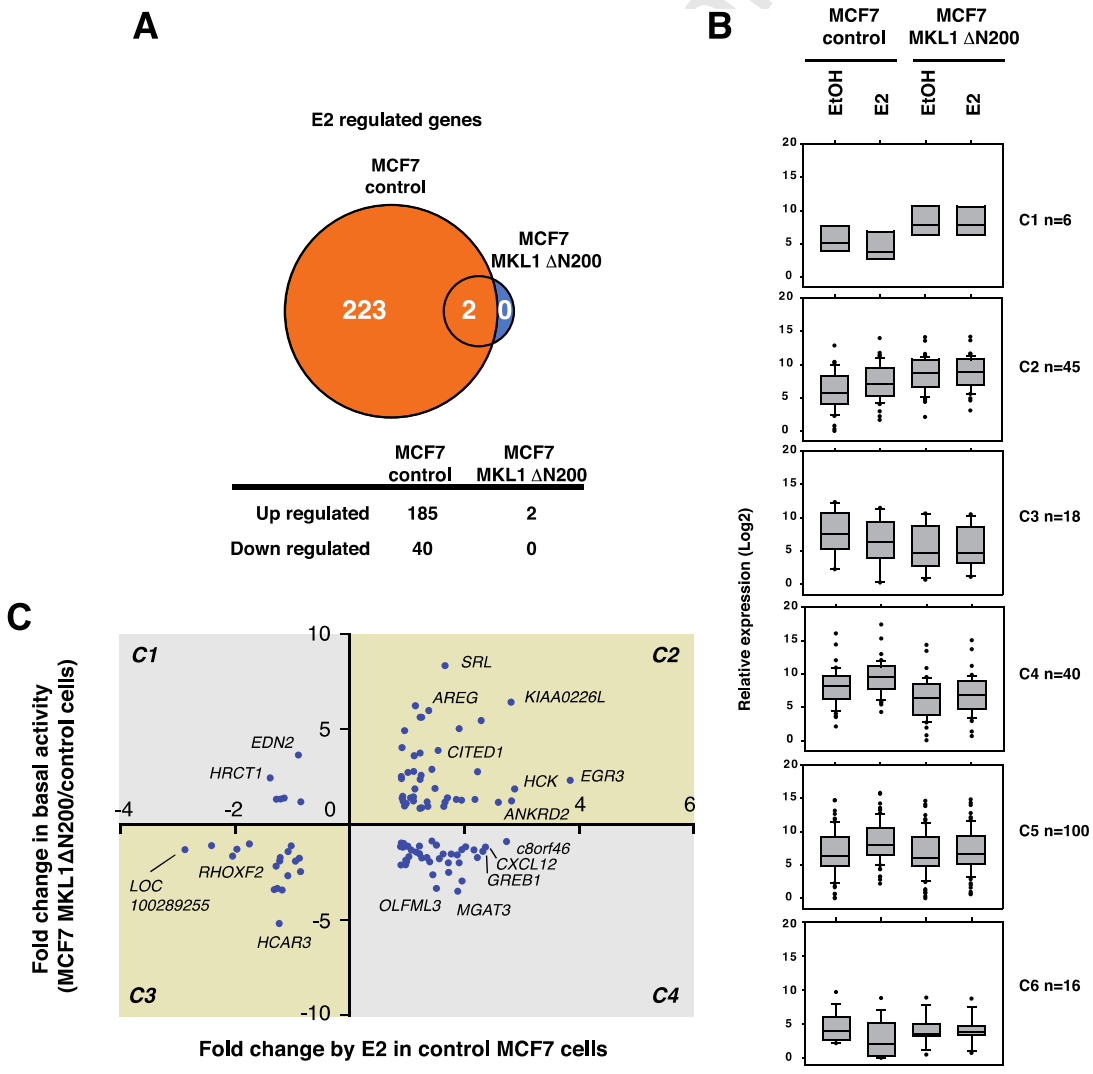

Fig. 4. E2 modulation of transcription is abrogated in MKL1 ΔN200 MCF7 cells. E2-regulated genes were identified in control and MKL1 ΔN200 MCF7 cells through microarray analysis. Cells were treated for 4h with 10 nM E2 or EtOH as a control. (A) Venn diagram of E2-regulated genes [showing P<0.05 and abs(FC)>1.8] in control and MKL1 ΔN200 MCF7 cells. (B) The 225 E2-regulated genes [P<0.05 and abs(FC)>1.8] were classified into 6 clusters (C1 to C6) according to the variations in their basal activity in MKL1 ΔN200 MCF7 cells [P<0.01 and abs(FC)>4]. Box plots represent the average expression level of the genes for each category in control and MKL1 ΔN200 MCF7 cells, treated or not with E2. (C) For the 109 genes that lose their response to E2 and presented significant variations in their basal activity in MKL1 ΔN200 MCF7 cells, we represented their changes in expression against their fold change in expression by E2 in control cells (C1-C4).

3.5. Nuclear accumulation of MKL1 in MCF7 cells impacts ERα cistrome

We next sought to determine whether the abrogation of gene responses to E2 observed in MCF7 cells expressing the MKL1 ΔN200 protein was correlated to an altered mobilization of ERα to its binding-sites. To this purpose, we treated control and MKL1 ΔN200 expressing cells with E2 or ethanol vehicle for 50 min, a time point adequate for determining representative direct sites of ERα binding to chromatin genome-wide [49], and subjected the prepared chromatin to ChIP-Seq as previously [36]. Bioinformatic treatment of these data included a filtration of the identified ERBSs against regions referenced as repetitive and sources of ChIP-Seq biases as well as against regions heavily duplicated/remodeled within MCF7 cells genome (see the Materials and Methods section as well as **Fig. S5**). The number of ERBSs retained before and after these filtering steps is given within **Table S10.** To ascertain the elimination of a maximum of false-positive regions, we measured the mean enrichment of ERα ChIP-Seq signal at ERBSs determined at different *P*-values, and subsequently selected those for which the signal/noise exceeded a 2-fold ratio (see **Fig. S5**). The Venn diagrams presented within **Fig. 5A** illustrate the overlap between the different set of ERBSs identified in each cell lines in the presence of absence of E2 at these optimal *P*-values. Mean ChIP-Seq signals measured on each specific subset of ERBSs are illustrated on the bottom of each Venn and confirm their selectivity (**Fig. 5B**).

In both cell lines, the number of common ERBSs found in EtOH and E2 conditions was relatively low (less than 5% or 1% of the ERBSs bound by ERα in the presence of E2 in control or MKL1 ΔN200 MCF7 cells, respectively). Interestingly, ERα cistromes included 6,237 or 2,658 ERBSs in E2-treated and 1,439 and

454 ERBSs in absence of hormone in control or MKL1 ΔN200 MCF7 cells, respectively. These observations indicate that the expression of the constitutive MKL1 ΔN200 protein alters ERα cistrome and induces a massive drop in the number of ERBSs, regardless of the presence of ligand. In addition, the overlaps between the cistromes of ERα in each cell line are relatively poor (**Fig. 5A**): only 1 ERBS in the absence of ligand and 367 in the presence of E2. This indicates that some reprogramming of ER binding on the genome had further occurred following the expression of the MKL1 ΔN200 protein. Importantly, using cistromes determined at less or more stringent *P*-values raised similar conclusions towards these overlaps (see **Fig. S6**). Hence, a maximum of 2% of the ERBSs identified in EtOH-treated control cells were common with those identified in similarly treated MKL1 ΔN200 MCF7 cells. The overlap reached 32% at low-stringency for E2 treated cells (see **Fig. S6**). To stress the robustness of our analysis, we performed ChIP-qPCR experiments on subsets of categorized ERBSs. Results obtained from these experiments are summarized in part of **Fig. 6**, and confirm that 100 % of the 4 lost and 4 gained tested ERBS recapitulate the expected profiles of enrichment. Interestingly, we also observed that the mobilization of ERα on common ERBSs located at the vicinity of E2 regulated genes such as *GREB1* was also strongly reduced in MKL1 ΔN200 MCF7 cells. Similarly, these ChIP-qPCR experiments evidenced a reduced or absent recruitment of ERα on distant enhancers establishing chromatin loops (as extracted from the ChiA-PET data from Fullwood et al., 2009 [50]) with the promoter of the two genes which are still regulated by ERα in MCF7 cells expressing the constitutive version of MKL1: *GPR68a* and *IFITM10a*.

To assess whether this reprogramming of ERα binding has a direct functional influence on MCF7 cell biology, we checked whether genes putatively regulated by these ERBSs share specific or similar annotations. We therefore applied GREAT on our data (http://great.stanford.edu/) [51], and found a number of associations of the ERα cistrome in MKL1 ΔN200 MCF7 cells with genes involved in EGF and RAS pathways. This was especially striking in absence of hormone (see **Fig. S7**) and congruent with our previous observations that MAP kinase signaling pathway is boosted in MKL1 ΔN200 MCF7 cells [28] (**Fig. S1B**). Therefore, in regard of these results, we analyzed by quantitative RT-PCR the expression profile of some E2-regulated genes from the clusters C1, C2 and C4 in MCF7 MKL1 ΔN200 and control cells after inhibition of HER1 pathway by the erlotinib drug. As shown in **Fig. S8**, the expression of the tested genes of cluster C2 (*EGR3* and *AREG*) was clearly inhibited in both cell lines after erlotinib treatment. However, it should be noted that erlotinib does not restore E2-dependent gene regulation and sensitivity to antiestrogen in MKL1 ΔN200 MCF7 cells.

We next investigated whether these specific cistromes could reflect the engagement of ERα on different type of DNA sequences. As visible from the motifs analysis summarized within **Table S11**, EREs are the first motifs found in each cistromes except within sites bound by ERα in the absence of E2 in MKL1 ΔN200 MCF7 cells. This again points to the conclusion that the very limited cistrome of ERα in this condition has probably specific properties. Accordingly, whilst the overlap of our ERα cistromes with the binding sites of other transcription factors determined in MCF7 cells (references in **Table S12**) did not evidence the existence of a preferential cofactor for the specific ERBSs from MKL1 ΔN200 MCF7 cells. Motifs recognized by proteins allowing an indirect recruitment of ERα such as AP1 (JUN/FOS) were also identified in these cells. However, the ERα cistrome in these cells in the absence of E2 was found particular as it did not cluster with the others (**Fig. 5C**). It can be noted that the ERBSs of these untreated cells present a depletion of GATA3 binding sites and the maintenance of enrichment in FOXA1. We further evaluated the overlap of the ERBSs specifically lost or created in MKL1 ΔN200 MCF7 cells with the cistromes of other transcription factors and some chromatin marks determined by others in MCF7 cells. Interestingly, these analyses summarized within the **Fig. S9** indicated that the novel ERBSs may exhibit a relative open chromatin conformation as revealed by a little accessibility to DNase I digestion in MCF7 cells. However, these sites may not be fully functional since they are not overlapping with FOXA1 or GATA3 cistromes (**Fig. S9**). Since MKL1 is a coactivator of SRF, we envisioned that the specific ERBSs from MKL1 ΔN200 MCF7 cells could be enriched in SRF binding sites. However, our motif analysis and search using known PSSM matrices (data not shown) showed that it is not the case.

These conclusions led us to hypothesize that the loss of any estrogenic regulation in the MKL1 ΔN200 cells could be a consequence of the impacted mobilization of ERα onto chromatin in the absence of ligand. We therefore interrogated the ERα cistromes characterized in control and MKL1 ΔN200 MCF7 cells to determine whether they may correlate with specific variations of gene basal activities preventing their estrogenic response. To do so, we first identified the closest ERBS from the TSS of the genes included in the 6 categories previously defined (**Fig. 4B** and **4C**). As shown within **Fig. 5D**, there was no obvious correlation between the variations in the basal transcriptional activity of a given gene category and either the conservation/gain or loss of their most proximal ERBS. For instance, genes with increased (C1 and C2) or decreased (C3 and C4) basal activity did not present coordinated changes in ERBS proximity significantly different from control genes with no changes in basal activity (C5 and C6). On the other hand, genes from the C2 and C4 categories of genes up-regulated by E2 in control cells seemed to conserve their more

proximal ERBS in MKL1 ΔN200 MCF7 cells more frequently than the other categories. In the opposite, down-regulated genes (C1, C3 and C6) have a tendency to gain an ERBS at their vicinity. These observations led us to check whether the levels of mobilization of ERα rather than the existence of the ERBS in itself could correlate better with the transcriptional activity. We therefore retrieved the mean ChIP-Seq signal from the conserved proximal ERBSs of the categorized genes, as well as the lost ones as a control. These analyses, summarized within **Fig. 5E** indicate that the mobilization of ERα on all conserved ERBSs from all categories is significantly reduced in the presence of E2 in MKL1 ΔN200 MCF7 cells. This is also the case in the absence of E2, except in the C6 category.

In summary our comparative analysis of ERα cistrome in MCF7 and MCF7 MKL1 ΔN200 cells indicates that ERα binding on the MCF7 cell's genome is strongly impaired by the cellular context imposed by the expression of the mutant MKL1 protein. This reprogramming involves a massive loss of ERBSs and a diminished recruitment of ERα on conserved ERBSs that may explain at least partly the loss of estrogenic transcriptional regulations. This is certainly partly associated with the loss of ERα protein amounts in MKL1 ΔN200 cells, but novel ERBSs also appear in these cells although their association with a particular physiological function remains unclear except for the EGF and RAS pathways.

Journal Pre-proof

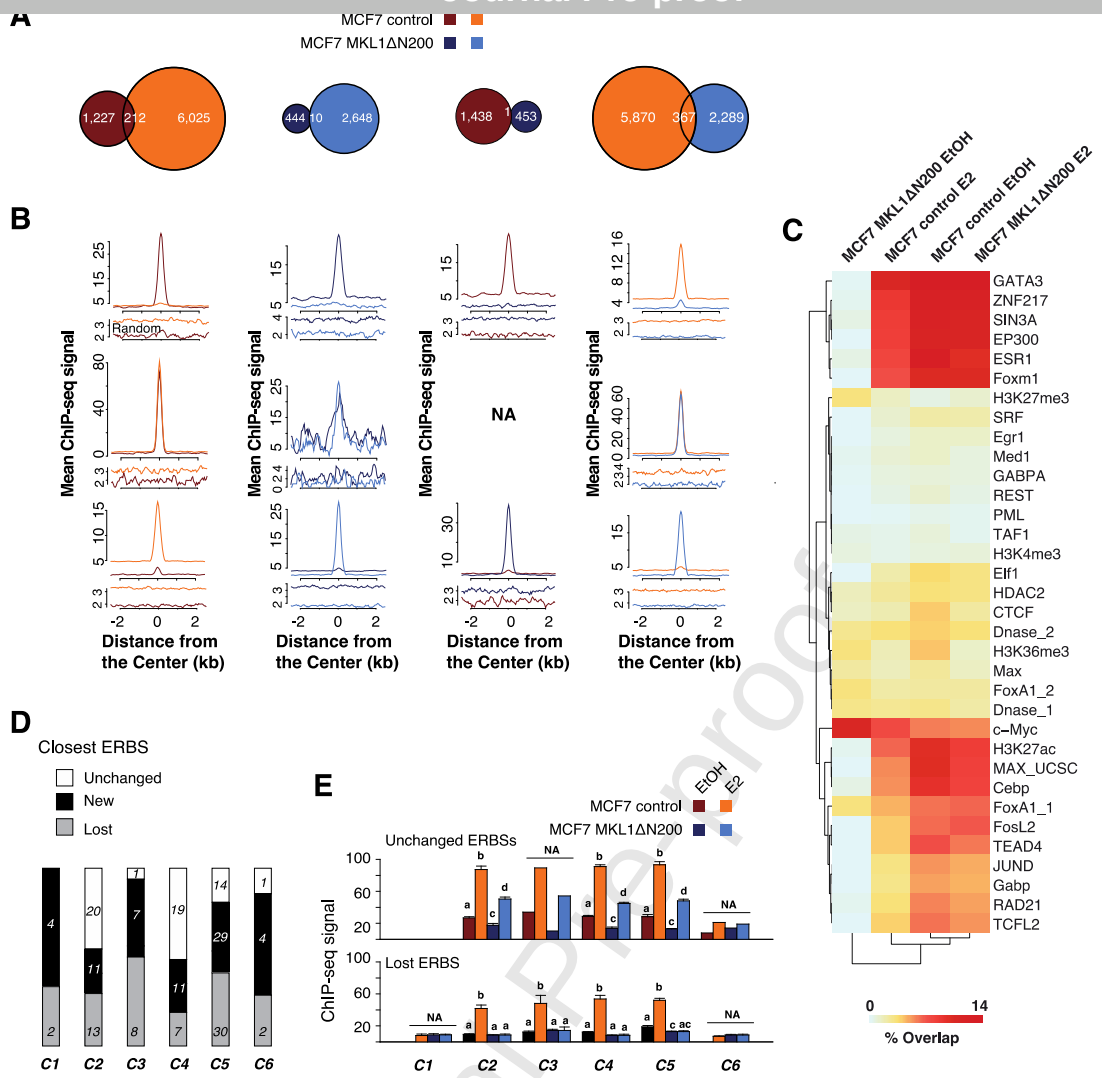

Fig. 5. ERα cistrome is affected by the expression of MKL1 ΔN200 protein in MCF7 cells. (A) Venn diagrams summarizing the overlaps of genomic regions bound by ERα in control MCF7 cells or MCF7 cells expressing the MKL1 ΔN200 following a 50 min treatment with either E2 or ethanol (EtOH) as vehicle control, as determined from ChIP-Seq experiments. (B) The ERα ChIP-Seq signals were aligned and averaged within a -2.5/+2.5 kbp window centered on ERBSs belonging to categories illustrated in the Venns on the upper panel (A). Upper and lower panels correspond to specific ERBSs to each of the two populations analyzed on the venn diagrams while the middle panel corresponds to overlap genomic regions of ERα binding. NA stands for non-applicable, since only one ERBS is common between the ERα cistromes determined in the two cell lines in the absence of E2. (C) Hierarchical clustering of the % of overlap of ERα cistromes in control and MKL1 ΔN200 MCF7 cells with the binding sites of other transcription factors or enriched region of histone marks previously determined in MCF-7 cells (see references in Table S11). (D) To correlate this change of ERα cistrome and our transcriptome analysis, we first identified the closest ERBSs from the TSSs

of the 223 genes that were not anymore regulated by E2 in MKL1 ΔN200 MCF7, present in either control or MKL1 ΔN200 MCF7 cells. We used the categories defined previously in Fig. 4. The stacked histogram shown illustrates the % of overlap between these ERBSs. (E) Graphs representing the mean ChIP-Seq signal obtained at the center of the ERBSs located at the vicinity of the TSSs of categorized genes in the different cells and conditions. The graph on the top represents values obtained on ERBSs which are common in control and or MKL1 ΔN200 MCF7 cells. The histogram at the bottom is shown as a control, illustrating the mean values on the ERBSs that disappeared upon expression of the MKL1 ΔN200 protein. Columns with different superscripts differ significantly ($p<0.05$, Student 's *t*-test). NA: n too low.

3.6. ERBSs enrichment in H3K27ac is altered in MCF7 MKL1 ΔN200 cells

We reasoned that the novel ERBSs identified in MCF7 MKL1 ΔN200 might not be functional in terms of chromatin remodeling required for transcriptional modulations. We therefore determined whether these ERBSs and variations in ERα mobilization on ERBSs in MCF7 MKL1 ΔN200 cells were associated with changes in chromatin structure around enhancers. We investigated the enrichment of ERBSs in dimethylated H3K4 (H3K4me2) and acetylated H3K27 acetylation (H3K27ac) in response to estrogenic treatment. Both chromatin marks are present at active enhancers and promoters, and H3K27ac is a major histone modification deposited at nucleosomes flanking enhancer elements by coactivators with histone acetyl activity (HAT) recruited by ERα and other transcription factors [52]. ChIP-qPCR experiments were performed on the same subsets of categorized ERBSs and with the same chromatin samples previously used to confirm ERα recruitment. As illustrated within the heatmap in **Fig. 6A**, the enrichment of all tested ERBSs in H3K4me2 was found independent of E2, as expected, in both cell lines. Importantly, the H3K4me2 levels were significantly lower in MCF7 MKL1 ΔN200 cells on the tested lost ERBSs (see **Fig. 6B** for the mean signals and statistics). In contrast, gained ERBSs did not present a differential enrichment in H3K4me2 depending upon the cell and/or treatment. This suggests that the gained ERBSs are genomic regions which are already poised for functionality in the absence of ERα, at least for those we tested. This was in line with the observed little overlap of these novel ERBSs with regions determined as having an open chromatin in native MCF7 cells (**Fig. S9**). H3K27ac enrichment at ERBS was extremely different between both cell lines with a clear decrease in common ERBSs, which was amplified in lost ERBSs. Importantly, although already present in MCF7 control cells within gained ERBSs there was a significant increase in the amounts of H3K27ac at these regions in MCF7 MKL1 ΔN200 cells. Interestingly, although insensitive to E2

in tested lost and gained ERBSs, 6 of the 7 common tested ERBSs showed an increased enrichment in H3K27ac in MCF7 MKL1 ΔN200 cells following E2 treatment, leading to a partial rescue of the levels of its enrichment when compared to control MCF7 cells (**Fig. 6A** and **6B**).

Altogether, these data indicate that gained ERBSs are, for the ones tested, already in a poised/prepared state and that the nuclear accumulation of the constitutively active form of MKL1 disturbs the H3K27 acetylation of ERBSs in a close association with the provoked changes in ERα mobilization.

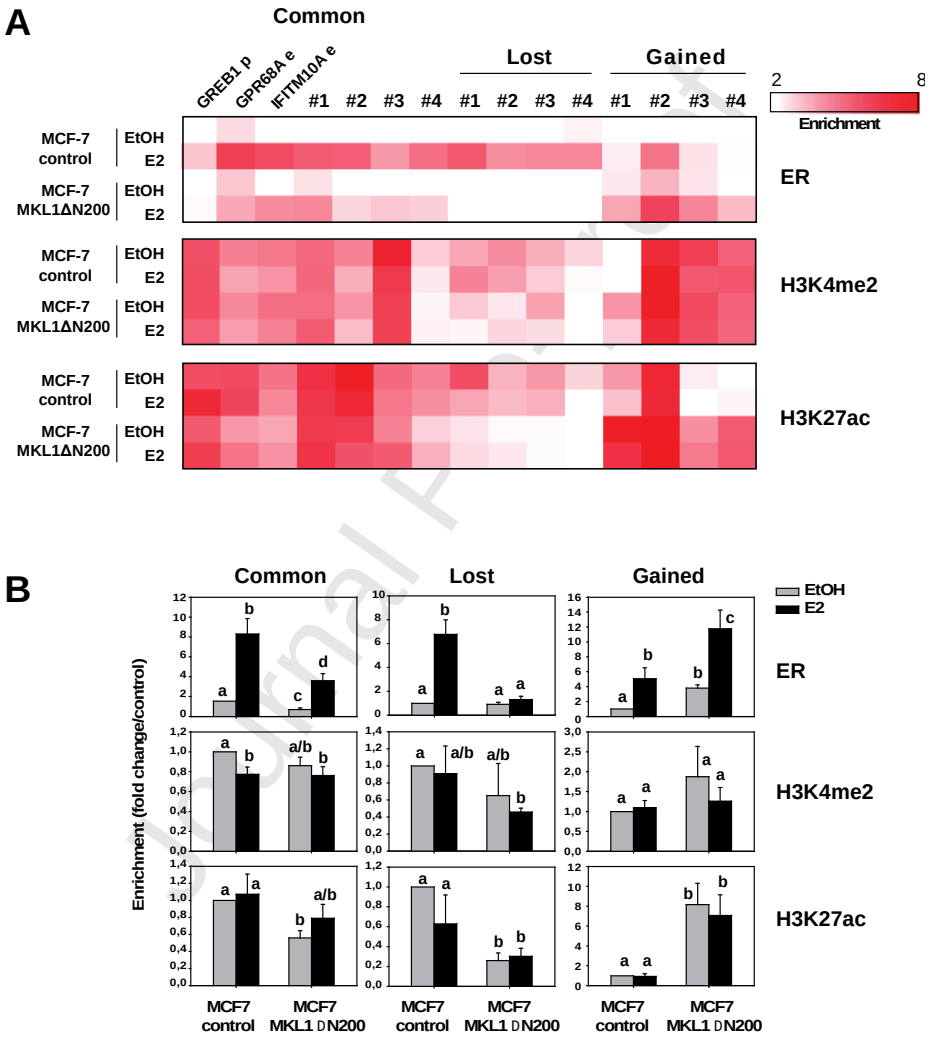

Fig. 6. Chromatin status of ERBSs in control and MKL1 ΔN200 MCF7 cells. (A) Heatmap summarizing data obtained in ChIP-qPCR experiments that evaluated ERα recruitment and H3K4me2 and H3K27ac enrichments on 7 genomic regions bound by ERα in both control and MKL1 ΔN200 MCF7 cells as well as on 4 lost and 4 gained ERBSs in MKL1 ΔN200 MCF7 cells. Amongst the common ERBSs, we evaluated ERα binding and chromatin modifications occurring at regions located within the promoter of the model estrogen-responsive *GREB1* gene (GREB1 p) and two enhancers regulating *GPR68A* or *IFITMA* genes. Cells were

treated for 50 min with 10 nM E2 or EtOH as a control. Data shown are mean of relative enrichment (*n*=5) normalized to an internal control (*CXCL12* intron). (B) For each ERBS, values were expressed in fold increase above the level measured in untreated control MCF7 cells and an average +/- SEM was then made for each category of ERBSs. Columns with different superscripts differ significantly ($p<0.05$, Student 's *t*-test).

4. Discussion

Thirty to 50% of recurrent tumors that arise from ERα-positive primary breast cancer patients fail to respond to endocrine therapy [8,9]. While the majority of these breast tumors retain ERα expression, high reduction or loss of ERα expression represents a non-negligible step in the progression from endocrine sensitive to resistance [19]. Notably, luminal B breast cancers, which generally express lower level of ERα, exhibit worse response to endocrine therapy. Understanding the underlying mechanisms of this progression is a major challenge towards the design of efficient hormone therapy-based treatments of breast cancers with reduced or ideally no relapses. We previously examined the processes controlling the tissue specific activity of ERα and identified the Rho/actin/MKL1 signaling pathway as a main actor, able to strongly inhibit the transcriptional capability of the receptor [30]. MKL1 is a master regulator of actin dynamic and cellular motile functions in many processes [20,21]. In breast tissue, MKL1 is vital in sustaining differentiation and function of mammary myoepithelial cells, accountable for ejection of the milk during lactation [22,23]. During tumor development, MLK1 can also promote malignancy by enhancing tumor cell invasion and metastatic dissemination [24]. We demonstrate in the present study that while MKL1 remains mainly cytoplasmic in estrogen-responsive, ERα-positive breast cancer cell lines, its nuclear localization is associated with basal-like phenotype in breast cancer cell lines and with endocrine resistance in a cohort of breast cancers. We further show that a provoked nuclear accumulation of MKL1 in ERα-positive breast cancer cells results in a genetic and phenotypic reprograming of luminal cancer cells to a mixed luminal/basal phenotype, conferring changes in ERα activity and the development of hormonal resistance.

As expected, the expression of a constitutively active form of MKL1 in MCF7 cells modulated the expression of numerous genes whose ontologies are associated with pathways involved in the regulation of actin cytoskeleton, focal adhesion, ECM-receptor interaction and cell migration. Importantly, the evaluation of the expression of subset of genes associated with specific breast cancer subgroup gene signature showed that the MKL1 ΔN200 expression triggered a partial shift from a luminal to a basal-like gene expression

profile. Notably, the expression of the pioneer factor GATA3 and ERα were down-regulated whilst that of the transcription factor FOXC1, a pivotal diagnostic marker for basal-like breast cancer [47], was induced. Of interest, FOXC1 is localized to the basal/myoepithelium in normal breast tissue and is particularly enriched in the luminal progenitor cell population, which is thought to be at the origin of basal-like tumors [53]. Markedly, the ectopic expression of FOXC1 was shown to induce a progenitor-like phenotype in differentiated mammary epithelial cells. Likewise, FOXC1 expression was associated with decreased or undetectable ERα expression in recurrent tumors from ERα-positive primary breast cancers, which were treated with endocrine therapy [54]. Amongst the possible mechanisms involved in this silencing of ERα expression, FOXC1 was shown to counteract GATA3 binding on ERα promoter region [54]. The switch between GATA3 and FOXC1 hence appears to be a good indicator of breast cancer luminal to basal-like reprograming [54,55]. Unlike GATA3 and ERα, FOXA1 not only remained expressed but even increased in MKL1 ΔN200 MCF7 cells. This may appear paradoxical because FOXA1 is generally associated, as GATA3 and ERα, with the luminal subtype [15]. However, recent studies evidenced an overexpression of FOXA1 in breast cancer metastases that are resistant to endocrine therapy, suggesting an altered role of FOXA1 in disease progression [14]. The presence of FOXA1 might also be related to the fact that the transition of MKL1 ΔN200 MCF7 cells from a luminal to a basal-like phenotype is not complete. Accordingly, we observed that MKL1 ΔN200 MCF7 cells still express some luminal markers such as cytokeratin 18. Interestingly, recent studies show that some luminal cell populations in normal human breast express myoepithelial/basal-like markers, which makes classification even more difficult [56].

Our microarray data further showed that the expression of MKL1 ΔN200 in MCF7 cells almost abolishes all E2-mediated transcriptional modulations. Of the 225 E2-regulated genes identified in MCF7 control cells, only two retained an E2-regulation in MKL1 ΔN200 MCF7 cells. The loss of E2-regulation was concomitant with a major overhaul in the basal expression of genes. For 28% of these genes, the change in their basal activity was in the same direction as the E2-response. Among these genes, we found *AREG (amphiregulin)*, the main growth factor mediating E2-driven epithelial proliferation in a paracrine fashion [57]. *AREG* was also shown to be involved in breast cancer progression, contributing to cell motility and invasion. The sharp increase of its expression in MKL1 ΔN200 MCF7 cells in a constitutive and E2-independent manner, associated with a higher expression of HER1 obviously contributes to the hormonal escape of these cells. For other E2-responsive genes such as the chemokine CXCL12, the changes in their basal expression were opposite to their normal E2-regulation. Here again, a shutdown of *CXCL12* expression associated with

a high expression of its receptor CXCR4, as observed in MKL1 ΔN200 MCF7 cells, is known to favor metastasis, cancer cells migrating *in vivo* to organs that express high level of CXCL12 [58]. Importantly, we did not observe any obvious correlation between the directions of changes of basal gene expression and the directions of E2-responses (up *vs.* down) for 72% of the genes that lose their responsiveness to the hormone. This point allows us to almost exclude the hypothesis that an increased ligand-independent activity of ERα on these genes might be the cause for a loss of their regulation by the hormone. Furthermore, we showed that changes in the basal expression of E2 target genes in MKL1 ΔN200 MCF7 cells were also insensitive to tamoxifen and ICI treatments, demonstrating unambiguously that the presence of a constantly active MKL1 in MCF7 induces ER-independent endocrine resistance.

ChIP-Seq experiments performed on endocrine resistant breast cancers and cell lines that retained ERα expression showed a clear increase in both number of ERBSs and the intensity of ER binding to these genomic regions [14]. Notably, the highest ERα chromatin binding signal intensities were observed in metastatic samples, suggesting a correlation with disease progression [14]. The estrogen responsive element (ERE) was the main DNA motif enriched in the ERBSs. It should be noticed that ligand-free constitutively activated mutant forms of ERα are often reported in endocrine resistant breast cancer metastases [59]. Because of the high ERα expression, these endocrine resistant cancer cells still remain in luminal breast cancer subtypes. Our data show that endocrine resistant breast cancer cells, which result from a massive MKL1 nuclear translocation, exhibit in contrary a reduced number of ERBSs generally associated with lower ERα-binding intensity. Besides a reduced overlap between the ERα cistromes identified in control and MKL1 ΔN200 MCF7 cells, we also identified novel ERBSs in cells expressing the MKL1 ΔN200 protein. This was particularly true in untreated cells for which the overlap was very weak. Interestingly, a number of genes located in the vicinity of these new ERBSs were associated with growth factor pathways, notably in untreated MKL1 ΔN200 MCF7 cells. This could be related to the sharp increase of expression of members of the EGF family (AREG as mentioned above, but also TGFα and HB-EGF) and their receptor in these cells. Interestingly, we show that the HER1 inhibitor erlotinib down regulates AREG expression suggesting the existence of a positive self-regulation loop in MCF7 between HER1 and its ligand, which becomes constitutive and E2-unregulated after nuclear translocation of MKL1 in the cells. Ross-Innes et al [14] previously showed that ERα positive breast cancer cell lines treated with a mitogenic cocktail present novel ERBSs at chromatin sites already bound by FOXA1 or to which FOXA1 was recruited in response to mitogenic stimulus. This phenomenon was also observed in ERα positive cancers associated

with poor prognosis or in ERα positive metastases. This supports the hypothesis that FOXA1 might mediate ERα-binding reprogramming in advanced diseases. Partially corroborating the hypothesis, the comparison of the new ERBSs identified in untreated MKL1 ΔN200 MCF7 cells with FOXA1 binding sites determined by ChIP-Seq in MCF7 show maintenance of FOXA1 enrichment. These gained ERBSs were also found to be contained within genomic regions exhibiting histone marks of chromatin poised for functionality. In contrast, depletion in GATA3 binding to chromatin was observed at these sites. Importantly, the reprogramming of ERBSs in untreated MKL1 ΔN200 MCF7 cells is therefore closely associated with the changes observed in the expression level of the two pioneer factors in these cells: down-regulation of *GATA3* and up-regulation of *FOXA1*. E2 treatment allows MKL1 Δ N200 MCF7 cells to regain enrichment profiles closer to those observed in control cells. The exact functional consequence of ERBS reprogramming in cells expressing the constitutively active form of MKL1 remains however poorly understood due to the lack of E2 transcriptional regulation in these cells.

Collectively, our study offers new mechanistic insights into ERα functional changes engaged during breast cancer progression particularly involving a nuclear accumulation of MKL1. Our work also implicates the targeting of the nuclear location of MKL1 as a potential therapeutic strategy for the treatment of endocrine-resistant and recurrent breast cancer.

Author contributions

G.F. conceived the project. C.J., T.F.-C., F.P., E.J., P.G. and G.F. conducted the experiments. T.F.-C., D.H., S.A. and R.M. analysed the microarray and ChIP-Seq data. C.J., M.M.C., and S.J. performed tissue microarrays. M.M. and D.M. contributed to the data analysis. T.F.-C., C.J., R.M. and G.F. wrote the manuscript with input from all authors.

Competing interests

The authors declare that they have no competing interests.

Acknowledgements

We thank the biosit Health genomics and H2P2-Histo pathology High precision core facilities of biogenouest and the IGBMC Micrroarray and Sequencing platform at Illkrich. This work was supported by the University of Rennes 1, Inserm, CNRS, and the Ligue Contre le Cancer.

References

[1] A. Skibinski, C. Kuperwasser, The origin of breast tumor heterogeneity, Oncogene. 34 (2015) 5309–5316. https://doi.org/10.1038/onc.2014.475.

[2] C.M. Perou, T. Sørlie, M.B. Eisen, M. van de Rijn, S.S. Jeffrey, C.A. Rees, J.R. Pollack, D.T. Ross, H. Johnsen, L.A. Akslen, O. Fluge, A. Pergamenschikov, C. Williams, S.X. Zhu, P.E. Lønning, A.L. Børresen-Dale, P.O. Brown, D. Botstein, Molecular portraits of human breast tumours, Nature. 406 (2000) 747–752. https://doi.org/10.1038/35021093.

[3] T. Sørlie, C.M. Perou, R. Tibshirani, T. Aas, S. Geisler, H. Johnsen, T. Hastie, M.B. Eisen, M. van de Rijn, S.S. Jeffrey, T. Thorsen, H. Quist, J.C. Matese, P.O. Brown, D. Botstein, P.E. Lønning, A.L. Børresen-Dale, Gene expression patterns of breast carcinomas distinguish tumor subclasses with clinical implications, Proc. Natl. Acad. Sci. U. S. A. 98 (2001) 10869–10874. https://doi.org/10.1073/pnas.191367098.

[4] N. Platet, A.M. Cathiard, M. Gleizes, M. Garcia, Estrogens and their receptors in breast cancer progression: a dual role in cancer proliferation and invasion, Crit. Rev. Oncol. Hematol. 51 (2004) 55–67. https://doi.org/10.1016/j.critrevonc.2004.02.001.

[5] K. Dahlman-Wright, V. Cavailles, S.A. Fuqua, V.C. Jordan, J.A. Katzenellenbogen, K.S. Korach, A. Maggi, M. Muramatsu, M.G. Parker, J.-A. Gustafsson, International Union of Pharmacology. LXIV. Estrogen receptors, Pharmacol. Rev. 58 (2006) 773–781. https://doi.org/10.1124/pr.58.4.8.

[6] C.K. Osborne, Steroid hormone receptors in breast cancer management, Breast Cancer Res. Treat. 51 (1998) 227–238.

[7] D.L. Wickerham, J.P. Costantino, V.G. Vogel, W.M. Cronin, R.S. Cecchini, L.G. Ford, N. Wolmark, The use of tamoxifen and raloxifene for the prevention of breast cancer, Recent Results Cancer Res. Fortschritte Krebsforsch. Progres Dans Rech. Sur Cancer. 181 (2009) 113–119.

[8] V.C. Jordan, B.W. O'Malley, Selective estrogen-receptor modulators and antihormonal resistance in breast cancer, J. Clin. Oncol. Off. J. Am. Soc. Clin. Oncol. 25 (2007) 5815–5824. https://doi.org/10.1200/JCO.2007.11.3886.

[9] R. Clarke, J.J. Tyson, J.M. Dixon, Endocrine resistance in breast cancer--An overview and update, Mol. Cell. Endocrinol. 418 Pt 3 (2015) 220–234. https://doi.org/10.1016/j.mce.2015.09.035.

[10] E.A. Musgrove, R.L. Sutherland, Biological determinants of endocrine resistance in breast cancer, Nat. Rev. Cancer. 9 (2009) 631–643. https://doi.org/10.1038/nrc2713.

[11] V.N.R. Gajulapalli, V.L. Malisetty, S.K. Chitta, B. Manavathi, Oestrogen receptor negativity in breast cancer: a cause or consequence?, Biosci. Rep. 36 (2016). https://doi.org/10.1042/BSR20160228.

[12] J.S. Carroll, C.A. Meyer, J. Song, W. Li, T.R. Geistlinger, J. Eeckhoute, A.S. Brodsky, E.K. Keeton, K.C. Fertuck, G.F. Hall, Q. Wang, S. Bekiranov, V. Sementchenko, E.A. Fox, P.A. Silver, T.R. Gingeras, X.S. Liu, M. Brown, Genome-wide analysis of estrogen receptor binding sites, Nat. Genet. 38 (2006) 1289–1297. https://doi.org/10.1038/ng1901.

[13] W.-J. Welboren, M.A. van Driel, E.M. Janssen-Megens, S.J. van Heeringen, F.C. Sweep, P.N. Span, H.G. Stunnenberg, ChIP-Seq of ERalpha and RNA polymerase II defines genes differentially responding to ligands, EMBO J. 28 (2009) 1418–1428. https://doi.org/10.1038/emboj.2009.88.

[14] C.S. Ross-Innes, R. Stark, A.E. Teschendorff, K.A. Holmes, H.R. Ali, M.J. Dunning, G.D. Brown, O. Gojis, I.O. Ellis, A.R. Green, S. Ali, S.-F. Chin, C. Palmieri, C. Caldas, J.S. Carroll, Differential oestrogen receptor binding is associated with clinical outcome in breast cancer, Nature. 481 (2012) 389–393. https://doi.org/10.1038/nature10730.

[15] K.M. Jozwik, J.S. Carroll, Pioneer factors in hormone-dependent cancers, Nat. Rev. Cancer. 12 (2012) 381–385. https://doi.org/10.1038/nrc3263.

[16] S. Badve, D.J. Dabbs, S.J. Schnitt, F.L. Baehner, T. Decker, V. Eusebi, S.B. Fox, S. Ichihara, J. Jacquemier, S.R. Lakhani, J. Palacios, E.A. Rakha, A.L. Richardson, F.C. Schmitt, P.-H. Tan, G.M. Tse, B. Weigelt, I.O. Ellis, J.S. Reis-Filho, Basal-like and triple-negative breast cancers: a critical review with an emphasis on the implications for pathologists and oncologists, Mod. Pathol. Off. J. U. S. Can. Acad. Pathol. Inc. 24 (2011) 157–167. https://doi.org/10.1038/modpathol.2010.200.

[17] E. Lim, F. Vaillant, D. Wu, N.C. Forrest, B. Pal, A.H. Hart, M.-L. Asselin-Labat, D.E. Gyorki, T. Ward, A. Partanen, F. Feleppa, L.I. Huschtscha, H.J. Thorne, kConFab, S.B. Fox, M. Yan, J.D.

French, M.A. Brown, G.K. Smyth, J.E. Visvader, G.J. Lindeman, Aberrant luminal progenitors as the candidate target population for basal tumor development in BRCA1 mutation carriers, Nat. Med. 15 (2009) 907–913. https://doi.org/10.1038/nm.2000.

[18] G. Molyneux, F.C. Geyer, F.-A. Magnay, A. McCarthy, H. Kendrick, R. Natrajan, A. Mackay, A. Grigoriadis, A. Tutt, A. Ashworth, J.S. Reis-Filho, M.J. Smalley, BRCA1 basal-like breast cancers originate from luminal epithelial progenitors and not from basal stem cells, Cell Stem Cell. 7 (2010) 403–417. https://doi.org/10.1016/j.stem.2010.07.010.

[19] T. Kuukasjärvi, J. Kononen, H. Helin, K. Holli, J. Isola, Loss of estrogen receptor in recurrent breast cancer is associated with poor response to endocrine therapy, J. Clin. Oncol. Off. J. Am. Soc. Clin. Oncol. 14 (1996) 2584–2589. https://doi.org/10.1200/JCO.1996.14.9.2584.

[20] F. Miralles, G. Posern, A.-I. Zaromytidou, R. Treisman, Actin dynamics control SRF activity by regulation of its coactivator MAL, Cell. 113 (2003) 329–342.

[21] G.C.T. Pipes, E.E. Creemers, E.N. Olson, The myocardin family of transcriptional coactivators: versatile regulators of cell growth, migration, and myogenesis, Genes Dev. 20 (2006) 1545–1556. https://doi.org/10.1101/gad.1428006.

[22] S. Li, S. Chang, X. Qi, J.A. Richardson, E.N. Olson, Requirement of a myocardin-related transcription factor for development of mammary myoepithelial cells, Mol. Cell. Biol. 26 (2006) 5797–5808. https://doi.org/10.1128/MCB.00211-06.

[23] Y. Sun, K. Boyd, W. Xu, J. Ma, C.W. Jackson, A. Fu, J.M. Shillingford, G.W. Robinson, L. Hennighausen, J.K. Hitzler, Z. Ma, S.W. Morris, Acute myeloid leukemia-associated Mkl1 (Mrtf-a) is a key regulator of mammary gland function, Mol. Cell. Biol. 26 (2006) 5809–5826. https://doi.org/10.1128/MCB.00024-06.

[24] S. Medjkane, C. Perez-Sanchez, C. Gaggioli, E. Sahai, R. Treisman, Myocardin-related transcription factors and SRF are required for cytoskeletal dynamics and experimental metastasis, Nat. Cell Biol. 11 (2009) 257–268. https://doi.org/10.1038/ncb1833.

[25] K.S. Purrington, S. Slager, D. Eccles, D. Yannoukakos, P.A. Fasching, P. Miron, J. Carpenter, J. Chang-Claude, N.G. Martin, G.W. Montgomery, V. Kristensen, H. Anton-Culver, P. Goodfellow, W.J. Tapper, S. Rafiq, S.M. Gerty, L. Durcan, I. Konstantopoulou, F. Fostira, A. Vratimos, P. Apostolou, I. Konstanta, V. Kotoula, S. Lakis, M.A. Dimopoulos, D. Skarlos, D. Pectasides, G. Fountzilas, M.W. Beckmann, A. Hein, M. Ruebner, A.B. Ekici, A. Hartmann, R. Schulz-Wendtland, S.P. Renner, W. Janni, B. Rack, C. Scholz, J. Neugebauer, U. Andergassen, M.P. Lux, L. Haeberle, C. Clarke, N. Pathmanathan, A. Rudolph, D. Flesch-Janys, S. Nickels, J.E. Olson, J.N. Ingle, C. Olswold, S. Slettedahl, J.E. Eckel-Passow, S.K. Anderson, D.W. Visscher, V.L. Cafourek, H. Sicotte, N. Prodduturi, E. Weiderpass, L. Bernstein, A. Ziogas, J. Ivanovich, G.G. Giles, L. Baglietto, M. Southey, V.-M. Kosma, H.-P. Fischer, GENICA Network, M.W.R. Reed, S.S. Cross, S. Deming-Halverson, M. Shrubsole, Q. Cai, X.-O. Shu, M. Daly, J. Weaver, E. Ross, J. Klemp, P. Sharma, D. Torres, T. Rüdiger, H. Wölfing, H.-U. Ulmer, A. Försti, T. Khoury, S. Kumar, R. Pilarski, C.L. Shapiro, D. Greco, P. Heikkilä, K. Aittomäki, C. Blomqvist, A. Irwanto, J. Liu, V.S. Pankratz, X. Wang, G. Severi, A. Mannermaa, D. Easton, P. Hall, H. Brauch, A. Cox, W. Zheng, A.K. Godwin, U. Hamann, C. Ambrosone, A.E. Toland, H. Nevanlinna, C.M. Vachon, F.J. Couch, Genome-wide association study identifies 25 known breast cancer susceptibility loci as risk factors for triple-negative breast cancer, Carcinogenesis. 35 (2014) 1012–1019. https://doi.org/10.1093/carcin/bgt404.

[26] I. Gurbuz, J. Ferralli, T. Roloff, R. Chiquet-Ehrismann, M.B. Asparuhova, SAP domain-dependent Mkl1 signaling stimulates proliferation and cell migration by induction of a distinct gene set indicative of poor prognosis in breast cancer patients, Mol. Cancer. 13 (2014) 22. https://doi.org/10.1186/1476-4598-13-22.

[27] S. Lindström, D.J. Thompson, A.D. Paterson, J. Li, G.L. Gierach, C. Scott, J. Stone, J.A. Douglas, I. dos-Santos-Silva, P. Fernandez-Navarro, J. Verghase, P. Smith, J. Brown, R. Luben, N.J. Wareham, R.J.F. Loos, J.A. Heit, V.S. Pankratz, A. Norman, E.L. Goode, J.M. Cunningham, M. deAndrade, R.A. Vierkant, K. Czene, P.A. Fasching, L. Baglietto, M.C. Southey, G.G. Giles, K.P. Shah, H.-P. Chan, M.A. Helvie, A.H. Beck, N.W. Knoblauch, A. Hazra, D.J. Hunter, P. Kraft, M. Pollan, J.D. Figueroa, F.J. Couch, J.L. Hopper, P. Hall, D.F. Easton, N.F. Boyd, C.M. Vachon, R.M. Tamimi, Genome-wide association study identifies multiple loci associated with both mammographic density and breast cancer risk, Nat. Commun. 5 (2014) 5303. https://doi.org/10.1038/ncomms6303.

[28] G. Kerdivel, A. Boudot, D. Habauzit, F. Percevault, F. Demay, F. Pakdel, G. Flouriot, Activation of the MKL1/actin signaling pathway induces hormonal escape in estrogen-responsive breast cancer cell lines, Mol. Cell. Endocrinol. 390 (2014) 34–44. https://doi.org/10.1016/j.mce.2014.03.009.

[29] G. Flouriot, G. Huet, F. Demay, F. Pakdel, N. Boujrad, D. Michel, The actin/MKL1 signalling pathway influences cell growth and gene expression through large-scale chromatin reorganization and histone post-translational modifications, Biochem. J. 461 (2014) 257–268. https://doi.org/10.1042/BJ20131240.

[30] G. Huet, Y. Mérot, F. Percevault, C. Tiffoche, J.-F. Arnal, N. Boujrad, F. Pakdel, R. Métivier, G. Flouriot, Repression of the estrogen receptor-alpha transcriptional activity by the Rho/megakaryoblastic leukemia 1 signaling pathway, J. Biol. Chem. 284 (2009) 33729–33739. https://doi.org/10.1074/jbc.M109.045534.

[31] G. Flouriot, C. Vaillant, G. Salbert, C. Pelissero, J.M. Guiraud, Y. Valotaire, Monolayer and aggregate cultures of rainbow trout hepatocytes: long-term and stable liver-specific expression in aggregates, J. Cell Sci. 105 (Pt 2) (1993) 407–416.

[32] R.C. Gentleman, V.J. Carey, D.M. Bates, B. Bolstad, M. Dettling, S. Dudoit, B. Ellis, L. Gautier, Y. Ge, J. Gentry, K. Hornik, T. Hothorn, W. Huber, S. Iacus, R. Irizarry, F. Leisch, C. Li, M. Maechler, A.J. Rossini, G. Sawitzki, C. Smith, G. Smyth, L. Tierney, J.Y.H. Yang, J. Zhang, Bioconductor: open software development for computational biology and bioinformatics, Genome Biol. 5 (2004) R80. https://doi.org/10.1186/gb-2004-5-10-r80.

[33] J.M. Wettenhall, G.K. Smyth, limmaGUI: a graphical user interface for linear modeling of microarray data, Bioinforma. Oxf. Engl. 20 (2004) 3705–3706. https://doi.org/10.1093/bioinformatics/bth449.

[34] G. Yu, L.-G. Wang, Y. Han, Q.-Y. He, clusterProfiler: an R package for comparing biological themes among gene clusters, Omics J. Integr. Biol. 16 (2012) 284–287. https://doi.org/10.1089/omi.2011.0118.

[35] J. Quintin, C. Le Péron, G. Palierne, M. Bizot, S. Cunha, A.A. Sérandour, S. Avner, C. Henry, F. Percevault, M.-A. Belaud-Rotureau, S. Huet, E. Watrin, J. Eeckhoute, V. Legagneux, G. Salbert, R. Métivier, Dynamic estrogen receptor interactomes control estrogen-responsive trefoil Factor (TFF) locus cell-specific activities, Mol. Cell. Biol. 34 (2014) 2418–2436. https://doi.org/10.1128/MCB.00918-13.

[36] G. Palierne, A. Fabre, R. Solinhac, C. Le Péron, S. Avner, F. Lenfant, C. Fontaine, G. Salbert, G. Flouriot, J.-F. Arnal, R. Métivier, Changes in Gene Expression and Estrogen Receptor Cistrome in Mouse Liver Upon Acute E2 Treatment, Mol. Endocrinol. Baltim. Md. 30 (2016) 709–732. https://doi.org/10.1210/me.2015-1311.

[37] B. Langmead, C. Trapnell, M. Pop, S.L. Salzberg, Ultrafast and memory-efficient alignment of short DNA sequences to the human genome, Genome Biol. 10 (2009) R25. https://doi.org/10.1186/gb-2009-10-3-r25.

[38] H. Li, B. Handsaker, A. Wysoker, T. Fennell, J. Ruan, N. Homer, G. Marth, G. Abecasis, R. Durbin, 1000 Genome Project Data Processing Subgroup, The Sequence Alignment/Map format and SAMtools, Bioinforma. Oxf. Engl. 25 (2009) 2078–2079. https://doi.org/10.1093/bioinformatics/btp352.

[39] J. Feng, T. Liu, B. Qin, Y. Zhang, X.S. Liu, Identifying ChIP-seq enrichment using MACS, Nat. Protoc. 7 (2012) 1728–1740. https://doi.org/10.1038/nprot.2012.101.

[40] T. Liu, J.A. Ortiz, L. Taing, C.A. Meyer, B. Lee, Y. Zhang, H. Shin, S.S. Wong, J. Ma, Y. Lei, U.J. Pape, M. Poidinger, Y. Chen, K. Yeung, M. Brown, Y. Turpaz, X.S. Liu, Cistrome: an integrative platform for transcriptional regulation studies, Genome Biol. 12 (2011) R83. https://doi.org/10.1186/gb-2011-12-8-r83.

[41] T. Barrett, D.B. Troup, S.E. Wilhite, P. Ledoux, D. Rudnev, C. Evangelista, I.F. Kim, A. Soboleva, M. Tomashevsky, K.A. Marshall, K.H. Phillippy, P.M. Sherman, R.N. Muertter, R. Edgar, NCBI GEO: archive for high-throughput functional genomic data, Nucleic Acids Res. 37 (2009) D885-890. https://doi.org/10.1093/nar/gkn764.

[42] S. Lamouille, J. Xu, R. Derynck, Molecular mechanisms of epithelial-mesenchymal transition, Nat. Rev. Mol. Cell Biol. 15 (2014) 178–196. https://doi.org/10.1038/nrm3758.

[43] S.C. Stadler, C.D. Allis, Linking epithelial-to-mesenchymal-transition and epigenetic modifications, Semin. Cancer Biol. 22 (2012) 404–410. https://doi.org/10.1016/j.semcancer.2012.06.007.

[44] W.L. Tam, R.A. Weinberg, The epigenetics of epithelial-mesenchymal plasticity in cancer, Nat. Med. 19 (2013) 1438–1449. https://doi.org/10.1038/nm.3336.

[45] T. Sorlie, R. Tibshirani, J. Parker, T. Hastie, J.S. Marron, A. Nobel, S. Deng, H. Johnsen, R. Pesich, S. Geisler, J. Demeter, C.M. Perou, P.E. Lønning, P.O. Brown, A.-L. Børresen-Dale, D. Botstein, Repeated observation of breast tumor subtypes in independent gene expression data sets, Proc. Natl. Acad. Sci. U. S. A. 100 (2003) 8418–8423. https://doi.org/10.1073/pnas.0932692100.

[46] G.M. Bernardo, G. Bebek, C.L. Ginther, S.T. Sizemore, K.L. Lozada, J.D. Miedler, L.A. Anderson, A.K. Godwin, F.W. Abdul-Karim, D.J. Slamon, R.A. Keri, FOXA1 represses the molecular phenotype of basal breast cancer cells, Oncogene. 32 (2013) 554–563. https://doi.org/10.1038/onc.2012.62.

[47] P.S. Ray, J. Wang, Y. Qu, M.-S. Sim, J. Shamonki, S.P. Bagaria, X. Ye, B. Liu, D. Elashoff, D.S. Hoon, M.A. Walter, J.W. Martens, A.L. Richardson, A.E. Giuliano, X. Cui, FOXC1 is a potential prognostic biomarker with functional significance in basal-like breast cancer, Cancer Res. 70 (2010) 3870–3876. https://doi.org/10.1158/0008-5472.CAN-09-4120.

[48] J. Frasor, J.M. Danes, B. Komm, K.C.N. Chang, C.R. Lyttle, B.S. Katzenellenbogen, Profiling of estrogen up- and down-regulated gene expression in human breast cancer cells: insights into gene networks and pathways underlying estrogenic control of proliferation and cell phenotype, Endocrinology. 144 (2003) 4562–4574. https://doi.org/10.1210/en.2003-0567.

[49] K. Ovaska, F. Matarese, K. Grote, I. Charapitsa, A. Cervera, C. Liu, G. Reid, M. Seifert, H.G. Stunnenberg, S. Hautaniemi, Integrative analysis of deep sequencing data identifies estrogen receptor early response genes and links ATAD3B to poor survival in breast cancer, PLoS Comput. Biol. 9 (2013) e1003100. https://doi.org/10.1371/journal.pcbi.1003100.

[50] M.J. Fullwood, M.H. Liu, Y.F. Pan, J. Liu, H. Xu, Y.B. Mohamed, Y.L. Orlov, S. Velkov, A. Ho, P.H. Mei, E.G.Y. Chew, P.Y.H. Huang, W.-J. Welboren, Y. Han, H.S. Ooi, P.N. Ariyaratne, V.B. Vega, Y. Luo, P.Y. Tan, P.Y. Choy, K.D.S.A. Wansa, B. Zhao, K.S. Lim, S.C. Leow, J.S. Yow, R. Joseph, H. Li, K.V. Desai, J.S. Thomsen, Y.K. Lee, R.K.M. Karuturi, T. Herve, G. Bourque, H.G. Stunnenberg, X. Ruan, V. Cacheux-Rataboul, W.-K. Sung, E.T. Liu, C.-L. Wei, E. Cheung, Y. Ruan, An oestrogen-receptor-alpha-bound human chromatin interactome, Nature. 462 (2009) 58–64. https://doi.org/10.1038/nature08497.

[51] C.Y. McLean, D. Bristor, M. Hiller, S.L. Clarke, B.T. Schaar, C.B. Lowe, A.M. Wenger, G. Bejerano, GREAT improves functional interpretation of cis-regulatory regions, Nat. Biotechnol. 28 (2010) 495–501. https://doi.org/10.1038/nbt.1630.

[52] E. Calo, J. Wysocka, Modification of enhancer chromatin: what, how, and why?, Mol. Cell. 49 (2013) 825–837. https://doi.org/10.1016/j.molcel.2013.01.038.

[53] G.M. Sizemore, S.T. Sizemore, B. Pal, C.N. Booth, D.D. Seachrist, F.W. Abdul-Karim, T. Kume, R.A. Keri, FOXC1 is enriched in the mammary luminal progenitor population, but is not necessary for mouse mammary ductal morphogenesis, Biol. Reprod. 89 (2013) 10. https://doi.org/10.1095/biolreprod.113.108001.

[54] Y. Yu-Rice, Y. Jin, B. Han, Y. Qu, J. Johnson, T. Watanabe, L. Cheng, N. Deng, H. Tanaka, B. Gao, Z. Liu, Z. Sun, S. Bose, A.E. Giuliano, X. Cui, FOXC1 is involved in ERα silencing by counteracting GATA3 binding and is implicated in endocrine resistance, Oncogene. 35 (2016) 5400–5411. https://doi.org/10.1038/onc.2016.78.

[55] D. Tkocz, N.T. Crawford, N.E. Buckley, F.B. Berry, R.D. Kennedy, J.J. Gorski, D.P. Harkin, P.B. Mullan, BRCA1 and GATA3 corepress FOXC1 to inhibit the pathogenesis of basal-like breast cancers, Oncogene. 31 (2012) 3667–3678. https://doi.org/10.1038/onc.2011.531.

[56] S. Santagata, A. Thakkar, A. Ergonul, B. Wang, T. Woo, R. Hu, J.C. Harrell, G. McNamara, M. Schwede, A.C. Culhane, D. Kindelberger, S. Rodig, A. Richardson, S.J. Schnitt, R.M. Tamimi, T.A. Ince, Taxonomy of breast cancer based on normal cell phenotype predicts outcome, J. Clin. Invest. 124 (2014) 859–870. https://doi.org/10.1172/JCI70941.

[57] J. McBryan, J. Howlin, S. Napoletano, F. Martin, Amphiregulin: role in mammary gland development and breast cancer, J. Mammary Gland Biol. Neoplasia. 13 (2008) 159–169. https://doi.org/10.1007/s10911-008-9075-7.

[58] K.E. Luker, G.D. Luker, Functions of CXCL12 and CXCR4 in breast cancer, Cancer Lett. 238 (2006) 30–41. https://doi.org/10.1016/j.canlet.2005.06.021.

[59] V.C. Jordan, R. Curpan, P.Y. Maximov, Estrogen receptor mutations found in breast cancer metastases integrated with the molecular pharmacology of selective ER modulators, J. Natl. Cancer Inst. 107 (2015) djv075. https://doi.org/10.1093/jnci/djv075.

Suplementary data

Supplementary figures and part of supplementary tables:

Fig. S1, Impacts of the nuclear localization of MKL1. **Fig. S2**, Expression of MKL1ΔN200 protein in MCF7 cells induces changes in the expression of luminal-, basal-like- and HER2-breast cancer markers. **Fig. S3**,

Expression of MKL1ΔN200 protein in MCF7 cells impairs estrogenic transcriptional regulation. **Fig. S4**, Jasplakinolide treatment of MCF7 and T47D cells impairs estrogenic transcriptional regulation. **Fig. S5**, Determination of specific ERα cistromes. **Fig. S6**, Overlaps of ERα cistromes. **Fig. S7**, Annotations of ERα cistromes. **Fig. S8,** Impact of erlotinib treatment on estrogenic transcriptional regulation in MKL1ΔN200 and control cells. **Fig. S9**, Specific MKL1 ΔN200 MCF7 ERBSs do not overlap with the cistromes of other TFs determined in MCF7 cells. **Table S1**, Oligonucleotides used. **Table S2**, HTS statistics. **Table S10**, ER cistromes. **Table S11**, DNA motifs enriched within ERBSs. **Table S12**, Public dataset used. (PDF)

Table S3: BED file detailing ERα binding regions (ERBSs). (XLSX)

Table S4: Data on the 130 breast cancer patient samples. (XLSX)

Table S5: The complete list of differentially expressed genes between control and MKL1 ΔN200 MCF7 cells with their corresponding *P*-values and log2 fold changes. (XLSX)

Table S6: List of Gene Ontology terms and Kegg Pathways enriched in differentially expressed genes between control and MKL1 ΔN200 MCF7 cells. (XLSX)

Table S7: List of the selected genes, which have been associated to basal-like, luminal-like and HER2-overexpressing tumors, respectively. (XLSX)

Table S8: The complete list of genes with their corresponding *P*-values and log2 fold changes determined from E2-treated and untreated control MCF7 cells and MKL1 ΔN200 MCF7 cells. (XLSX)

Table S9: List of Gene Ontology terms and Kegg Pathways enriched in differentially expressed genes between E2-treated and untreated control MCF7 cells. (XLSX)

Journal Pre-proof

Declaration of interests

☐ X The authors declare that they have no known competing financial interests or personal relationships that could have appeared to influence the work reported in this paper.

☐The authors declare the following financial interests/personal relationships which may be considered as potential competing interests:

Journal Pre-proof

Highlights

Nuclear accumulation of MKL1 in luminal breast cancer cells impairs genomic activity of ERα and is associated with endocrine resistance

- MKL1 is a master regulator of actin dynamic and cellular motile functions.
- Nuclear translocation of MKL1 is associated with endocrine resistance.
- Nuclear translocation of MKL1 induces a mixed luminal/basal phenotype.
- Nuclear translocation of MKL1 suppresses estrogen-mediated control of gene expression.
- Nuclear translocation of MKL1 induces a profound reprogramming in ERα cistrome associated with a massive loss of ERα binding sites (ERBSs).

Journal Pre-proof

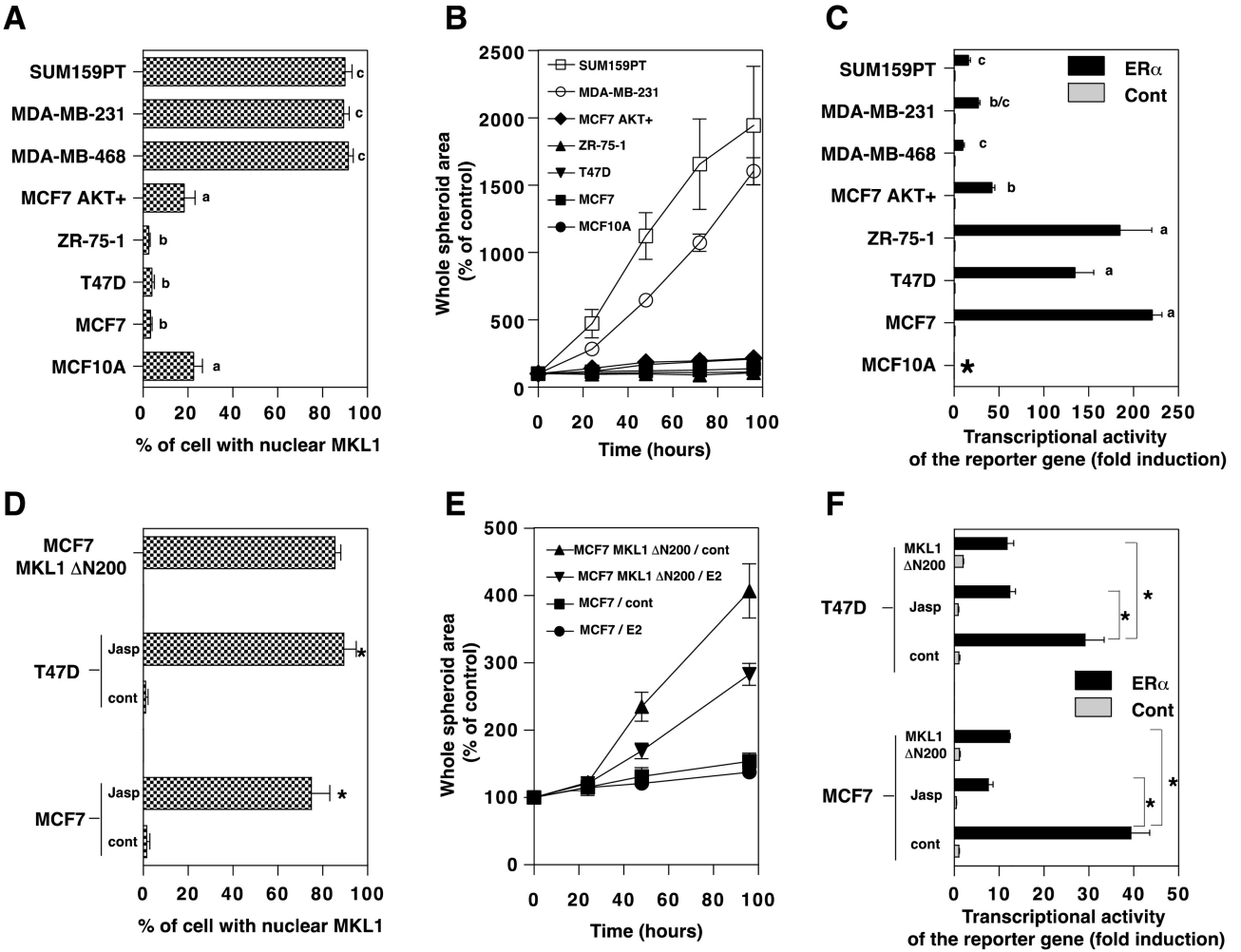
A
SUM159PT
MDA-MB-231
MDA-MB-468
MCF7 AKT+
ZR-75-1
T47D
MCF7
MCF10A
c
c
c
a
b
b
b
a
0 20 40 60 80 100
% of cell with nuclear MKL1
B
SUM159PT
MDA-MB-231
MCF7 AKT+
ZR-75-1
T47D
MCF7
MCF10A
Whole spheroid area (% of control)
2500
2000
1500
1000
500
0
0 20 40 60 80 100
Time (hours)
C
SUM159PT
MDA-MB-231
MDA-MB-468
MCF7 AKT+
ZR-75-1
T47D
MCF7
MCF10A
ERα
Cont
c
b/c
c
b
a
a
a
*
0 50 100 150 200 250
Transcriptional activity
of the reporter gene (fold induction)
D
MCF7
MKL1 ΔN200
T47D
Jasp
cont
MCF7
Jasp
cont
*
*
0 20 40 60 80 100
% of cell with nuclear MKL1
E
MCF7 MKL1 ΔN200 / cont
MCF7 MKL1 ΔN200 / E2
MCF7 / cont
MCF7 / E2
Whole spheroid area (% of control)
500
400
300
200
100
0
0 20 40 60 80 100
Time (hours)
F
T47D
MKL1 ΔN200
Jasp
cont
MCF7
MKL1 ΔN200
Jasp
cont
ERα
Cont
*
*
*
*
0 10 20 30 40 50
Transcriptional activity
of the reporter gene (fold induction)

Figure 1

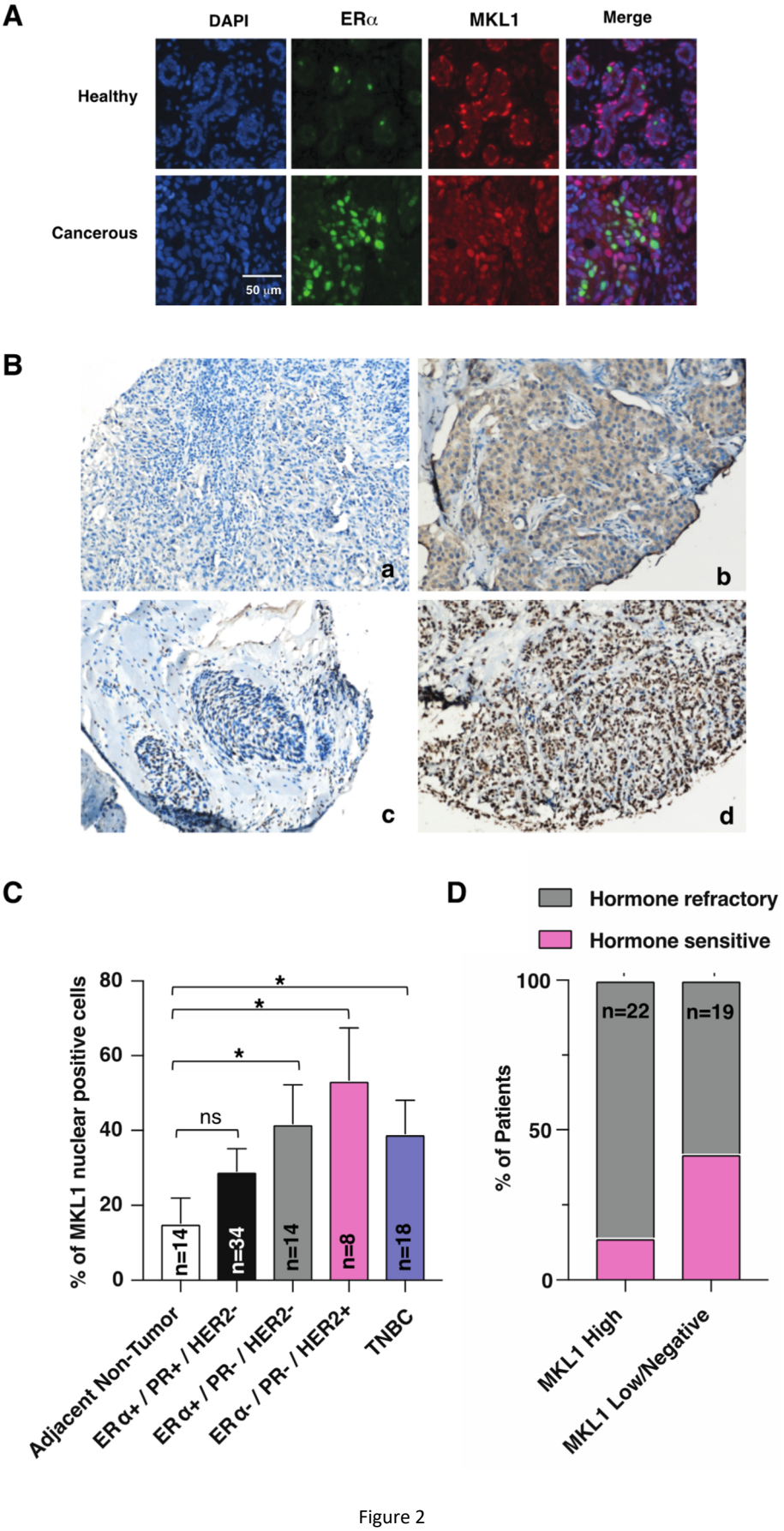
A
DAPI
ERα
MKL1
Merge
Healthy
Cancerous
50 µm
B
a
b
c
d
C
% of MKL1 nuclear positive cells
80
60
40
20
0
ns
*
*
*
n=14
n=34
n=14
n=8
n=18
Adjacent Non-Tumor
ERα+ / PR+ / HER2-
ERα+ / PR- / HER2-
ERα- / PR- / HER2+
TNBC
D
Hormone refractory
Hormone sensitive
% of Patients
100
50
0
n=22
n=19
MKL1 High
MKL1 Low/Negative

Figure 2

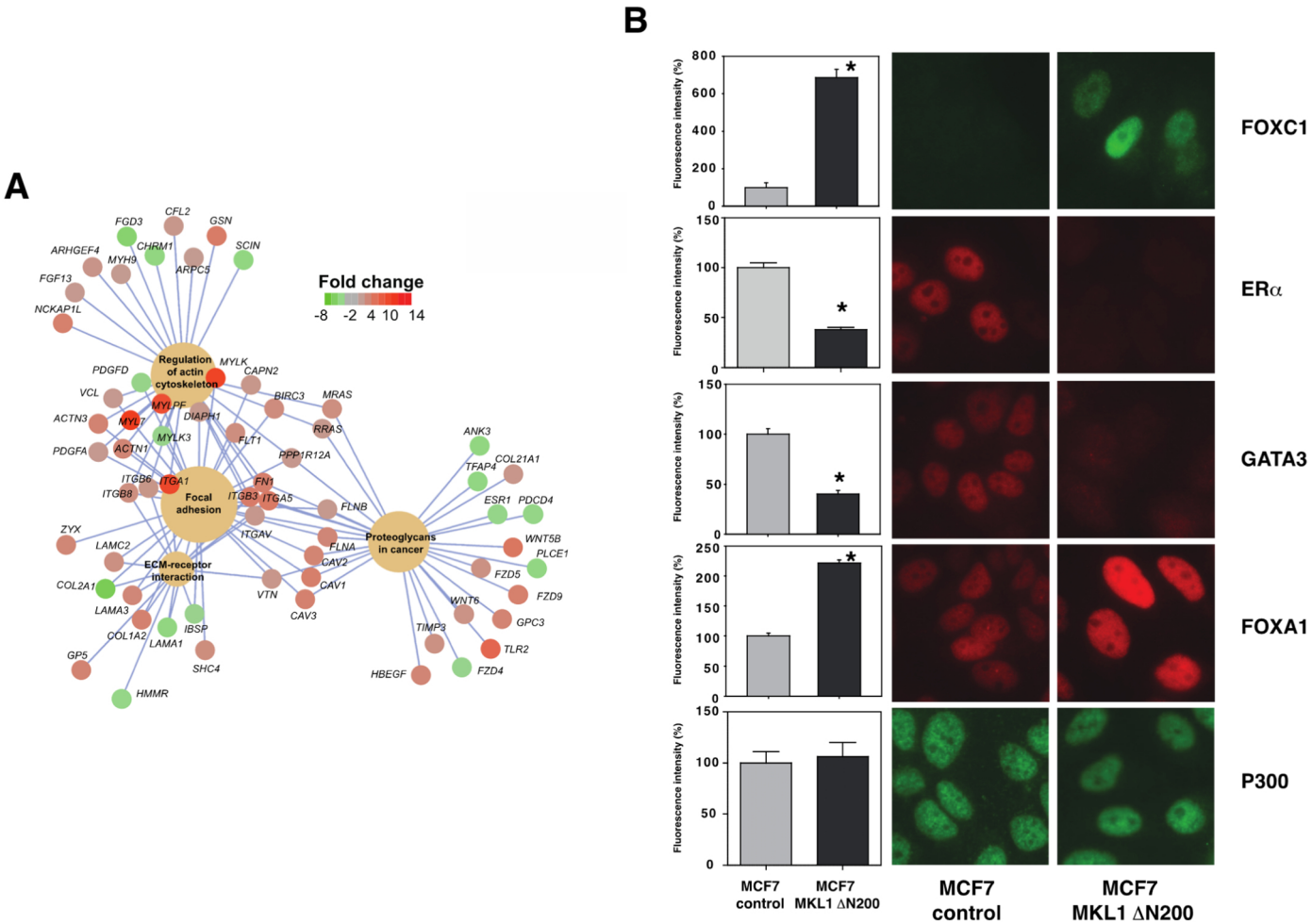
A
Fold change
-8 -2 4 10 14
Regulation of actin cytoskeleton
Focal adhesion
ECM-receptor interaction
Proteoglycans in cancer
FGD3
CFL2
GSN
ARHGEF4
CHRM1
SCIN
MYH9
ARPC5
FGF13
NCKAP1L
PDGFD
MYLK
CAPN2
VCL
BIRC3
MRAS
MYLPF
ACTN3
MYL7
DIAPH1
RRAS
MYLK3
FLT1
PDGFA
ACTN1
PPP1R12A
ITGB6
ITGA1
FN1
ITGB8
ITGB3
ITGA5
FLNB
ZYX
ITGAV
LAMC2
FLNA
CAV2
COL2A1
CAV1
VTN
LAMA3
CAV3
IBSP
COL1A2
LAMA1
GP5
SHC4
HMMR
ANK3
COL21A1
TFAP4
ESR1
PDCD4
WNT5B
PLCE1
FZD5
FZD9
WNT6
GPC3
TIMP3
TLR2
HBEGF
FZD4
B
Fluorescence intensity (%)
MCF7 control
MCF7 MKL1 ΔN200
FOXC1
ERα
GATA3
FOXA1
P300

Figure 3

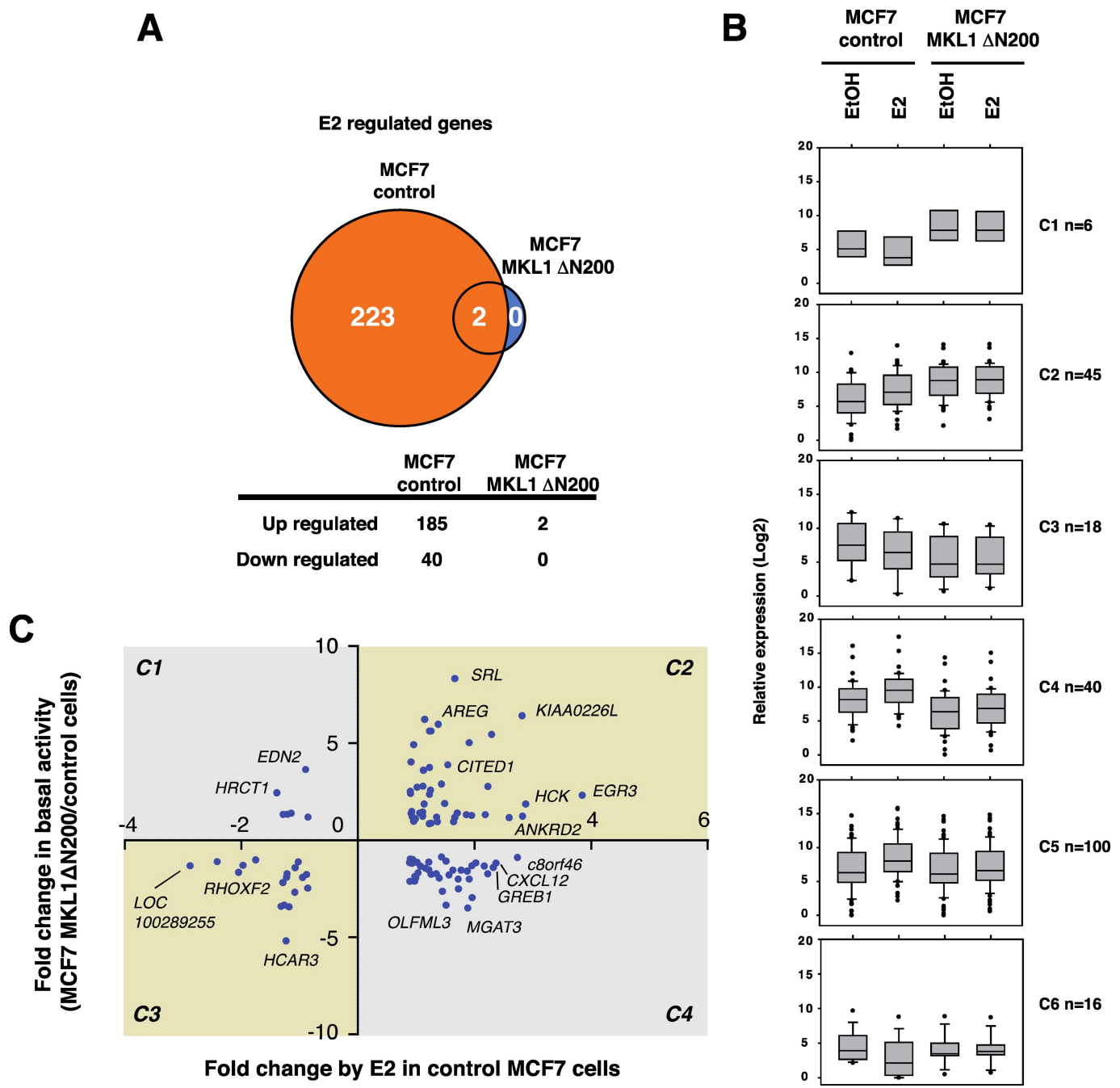
A
E2 regulated genes
MCF7 control
MCF7 MKL1 ΔN200
223
2
0
MCF7 control
MCF7 MKL1 ΔN200
Up regulated 185 2
Down regulated 40 0
B
MCF7 control
MCF7 MKL1 ΔN200
EtOH
E2
EtOH
E2
Relative expression (Log2)
C1 n=6
C2 n=45
C3 n=18
C4 n=40
C5 n=100
C6 n=16
C
C1
C2
C3
C4
SRL
AREG
KIAA0226L
EDN2
CITED1
HRCT1
HCK
EGR3
ANKRD2
c8orf46
CXCL12
GREB1
RHOXF2
LOC 100289255
OLFML3
MGAT3
HCAR3
Fold change in basal activity (MCF7 MKL1ΔN200/control cells)
Fold change by E2 in control MCF7 cells

Figure 4

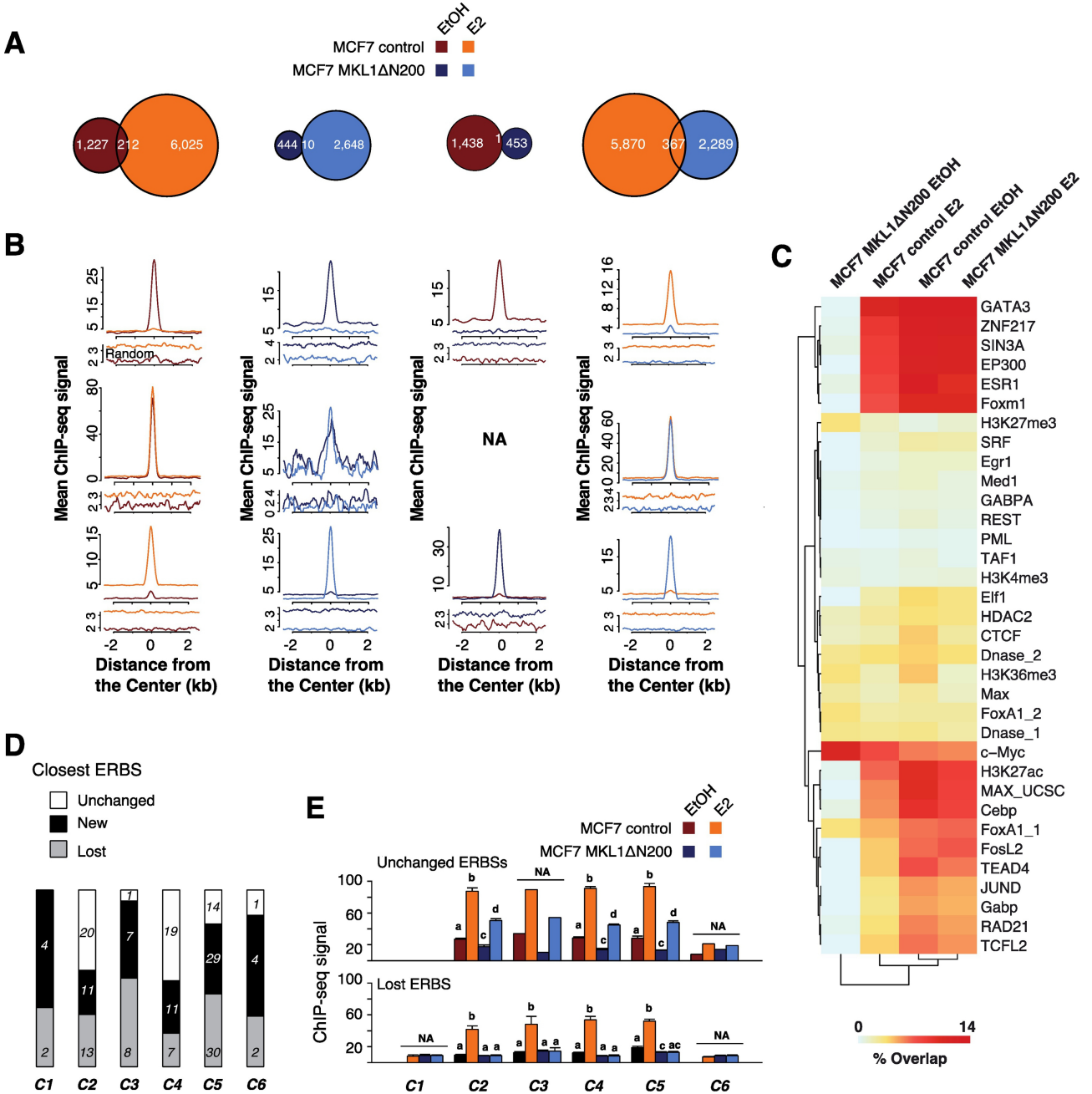
A
EtOH
E2
MCF7 control
MCF7 MKL1ΔN200
1,227
212
6,025
444
10
2,648
1,438
1
453
5,870
367
2,289
B
Random
Mean ChIP-seq signal
NA
Distance from the Center (kb)
C
MCF7 MKL1ΔN200 EtOH
MCF7 control E2
MCF7 control EtOH
MCF7 MKL1ΔN200 E2
GATA3
ZNF217
SIN3A
EP300
ESR1
Foxm1
H3K27me3
SRF
Egr1
Med1
GABPA
REST
PML
TAF1
H3K4me3
Elf1
HDAC2
CTCF
Dnase_2
H3K36me3
Max
FoxA1_2
Dnase_1
c–Myc
H3K27ac
MAX_UCSC
Cebp
FoxA1_1
FosL2
TEAD4
JUND
Gabp
RAD21
TCFL2
0
14
% Overlap
D
Closest ERBS
Unchanged
New
Lost
C1
C2
C3
C4
C5
C6
E
EtOH
E2
MCF7 control
MCF7 MKL1ΔN200
Unchanged ERBSs
Lost ERBS
ChIP-seq signal
NA

Figure 5

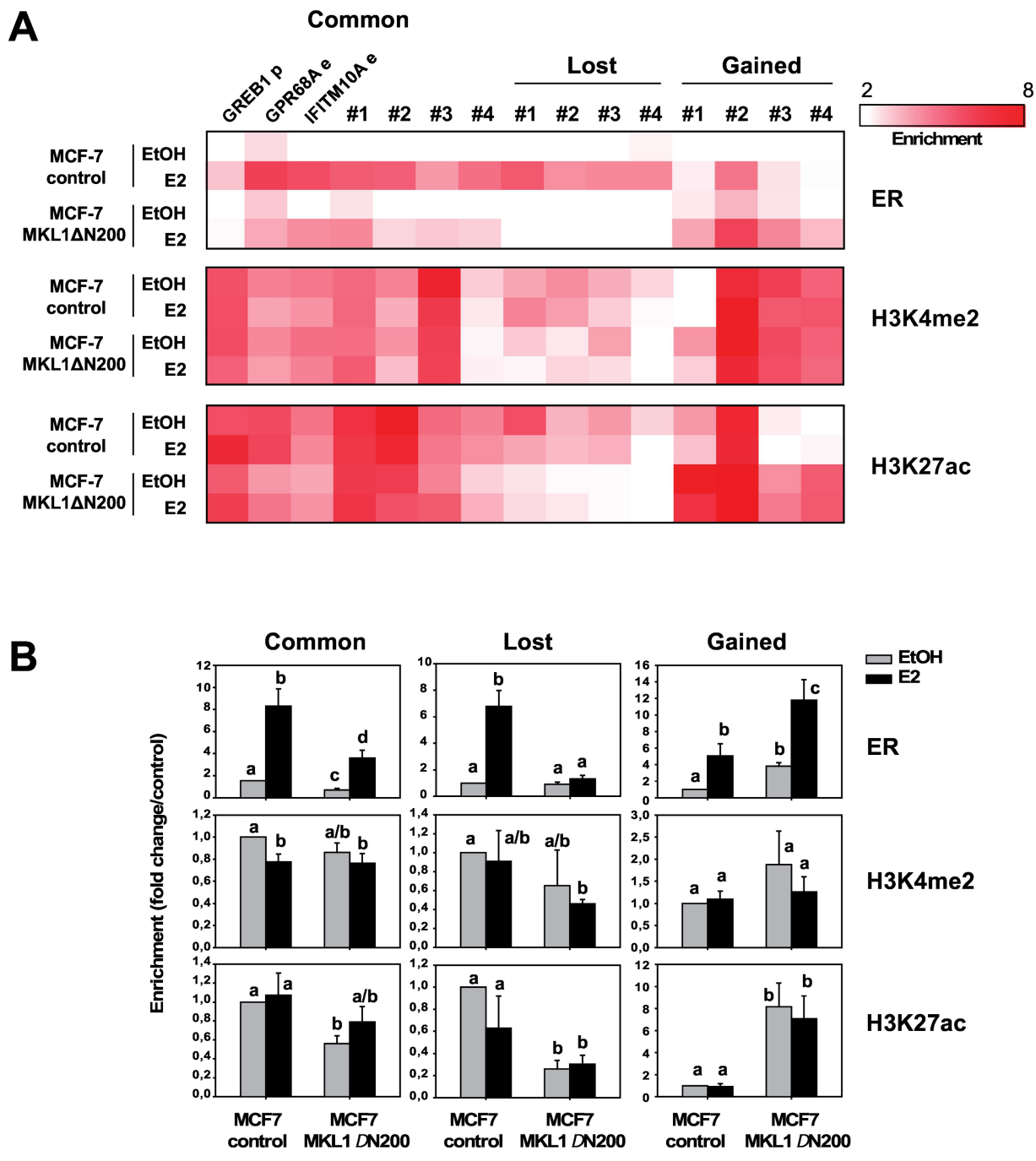
A
Common
Lost
Gained
GREB1 p
GPR68A e
IFITM10A e
#1
#2
#3
#4
2
8
Enrichment
MCF-7 control
MCF-7 MKL1ΔN200
EtOH
E2
ER
H3K4me2
H3K27ac
B
Common
Lost
Gained
EtOH
E2
Enrichment (fold change/control)
ER
H3K4me2
H3K27ac
MCF7 control
MCF7 MKL1 DN200

Figure 6